5 Water solvation dynamics in the bulk and in the hydration layer of proteins and self-assemblies

Biman Bagchi

Solid State and Structural Chemistry Unit, Indian Institute of Science, Bangalore 560 012, India

Water solvation dynamics of polar species both in the bulk and in the hydration layers of proteins and self-organized assemblies have been discussed. Recent studies have revealed that while water solvation dynamics in the bulk is ultrafast and is mostly complete within 1 ps, this can slow down by as much as 2–3 orders of magnitude in the hydration layers of these systems. In this Report we discuss not only the ultrafast solvation dynamics in bulk water and the slow dynamics in the hydration layers, but also the relevant experimental, theoretical and computer simulation studies on various aspects of water dynamics in self-assemblies and confined geometries.

1 Introduction

The study of the dynamics of solvation of a newly created ion or a dipole in polar liquids is now a well established method to obtain molecular level information about the collective solvent response (consisting of both orientational and translational motions) of the solvent molecules around the probe.[1–20] This area of study is hardly two decades old, yet it has already given rise to a large amount of new (even novel!) information which was not accessible before by other established means. This is still a very active area of research where new experimental techniques are still being developed, and theoretical and computer simulation studies are being actively pursued, with the emphasis now shifted to complex systems. In these studies, prime attention has been focused on water and aqueous systems. This is understandable because water, as a unique liquid, controls, in an essential way, the structure, function and reactivity of many natural and biological systems.[21–31] The aqueous medium helps the protein to attain its native or biologically active structure. The shell of water around DNA is essential for its function. In recent years, the study of solvation dynamics of a probe placed suitably near a biological surface in water has given rise to extremely important information about the nature of this water which is sometimes called "biological water".[21,11] However, the use of solvation dynamics in complex systems needed prior understanding of the phenomenon in simple liquids and especially in water.

DOI: 10.1039/b208505b

Many reviews have appeared in the literature on different aspects of solvation dynamics.[1–20] The focus of this review will be on solvation dynamics in water, both in the bulk and in aqueous protein solutions and self-organized assemblies. That is, studies devoted to other solvents will not be discussed. In addition, we shall attempt to give due importance to the large body of computer simulation studies that have been devoted to understanding water dynamics in complex systems.

In the initial period of development (from late 1970s to early 1990s), solvation dynamics studies were restricted (because of the limited temporal resolution then available to laser spectroscopy) to relatively slow dipolar liquids, like higher alcohols, propylene carbonate, *etc*.[32–41] The studies on water were carried out a bit later—even then the earlier studies could measure only the slow time constants.[2] Later studies found that 60–70% of polar solvation in water is completed in *less than* 50 fs.[42,43] In subsequent years, the method of solvation dynamics has been used extensively to study complex aqueous systems, like ionic liquids,[13] supramolecular assemblies in aqueous solutions (like micelles,[11,12,44–48] reverse micelles,[11,49–52] microemulsions,[11,52–54] lipid vesicles[11,55,56]), polymeric solutions,[11,57–61] aqueous protein[11,62–66] and DNA[67–69] solutions.

The usefulness of solvation dynamics as a tool for investigating liquid state dynamics lies in several factors. First, the probe can be located either in the bulk liquid or in the surface of a self-assembly or at the surface of a protein. Second, the method provides a vast temporal resolution, beginning from sub-nanosecond to a few femtoseconds. Third, it also offers a certain degree of spatial resolution because the contribution from nearest neighbour molecules is separated in time scale from the collective response, and is often the dominant term. Thus, if one knows the location of the probe, one can investigate the dynamics around the probe. In this regards, it is useful to contrast solvation dynamics with other techniques. Dielectric relaxation does not have adequate spatial resolution, as it probes the relaxation of the total dipole moment of the system. NMR techniques, such as NOE, have the adequate spatial resolution but do not have the temporal resolution (at least till now). This combination of wide temporal window with the spatial resolution, mentioned above, makes solvation dynamics a very useful tool in understanding dynamics of water in wide variety of complex systems.

The hydration shell that covers the surface of proteins, DNAs and micelles in an aqueous solution has been a subject of intense discussions in recent years.[9,11] Computer simulations have shown that water molecules in the hydration layer exhibit much anomalous behaviour, such as sub-diffusive translational diffusion and markedly non-exponential orientational relaxation. Solvation dynamics of probes located near the protein surface show a slow decay over a long time. This will be discussed here.

In addition to hydration dynamics at the surface of the biomolecules, considerable attention has been focussed on the solvation dynamics in self-assemblies such as micelles and reverse micelles, vesicles and lipid bi-layers. These systems show very slow solvation dynamics, often extending to a few ns. The origin of such a slow component is still a question of lively debate. The first observation of such a slow component was made in aqueous cyclodextrin (CDX) cavity by Vajda *et al.* who investigated solvation dynamics of coumarin in CDX solution.[70] This study motivated further theoretical[71] and experimental work.[11,12]

Thus, the focus of this Report is on the solvation dynamics of water both in the bulk and in the hydration layer of self-assemblies and bio-molecules. We shall also discuss recent advances in understanding the role of this biphasic water solvent response in various elementary relaxation processes, such as ionic mobility in aqueous electrolyte solutions and solvent dynamic effects on electron transfer reactions. Although the dominance of the ultrafast femtosecond component in water solvation dynamics did come somewhat as a surprise, it is the near *universal* presence of such an extremely fast component in many molecular liquids that has created a lot of interest and motivated new progresses in various directions. We shall try to articulate these in the present Report.

2 Natural dynamics of water

The understanding of the unusual features of the polar solvation dynamics in water requires understanding of the natural dynamics of water itself. The uniqueness of water originates largely from its hydrogen-bonded network. Each water molecule is capable of forming four hydrogen bonds. In two of them, the water molecule donates a hydrogen atom and in the two others, they accept hydrogen atoms. The average hydrogen bond coordination number of an individual water molecule is 3.5, which implies that water is a giant gel or cluster of water molecules. Not only the structure, but the dynamics of water also shows anomalous properties.

2.1 Vibrational dynamics

Vibrational dynamics of water not only provide a microscopic understanding of the motions of the atoms within a water molecule, but they also give us detailed information about *intermolecular* motions in the liquid. A water molecule is characterized by three intra-molecular vibrational modes—the symmetric and the anti-symmetric O–H stretches and the H–O–H bend. In the liquid state, these intra-molecular vibrational modes get shifted and mixed in a spectrum. The frequencies of these three modes for liquid water are 3656, 3755 and 1594 cm^{-1}, respectively.[72,73]

Because of the extensive hydrogen bond network, several low frequency intermolecular vibrational modes appear in liquid water. This is unique to liquid water and the low frequency modes have far reaching consequences in determining the collective dynamic response of liquid water. Among the low frequency modes, the mode near 650 cm^{-1} is assigned to the librational mode, the one near 200 cm^{-1} to the intermolecular vibrational mode and the one near 50 cm^{-1} to the hindered translational motion due to the caging of the water molecules.[74] The frequency spectrum of water in shown in Fig. 1. In addition to these three well-known intermolecular modes, studies have been carried out to probe the far infrared (FIR) low frequency spectrum in liquid water. Thrane *et al.* investigated the FIR spectrum from 2 to 35 cm^{-1} by using ultrashort THz pulses.[75] The absorption coefficient showed a continuous increase with frequency. The refractive index was found to decrease to about 2.2 at 35 cm^{-1}. There is no structure in such a low frequency range (IR studies confirm the presence of a weak

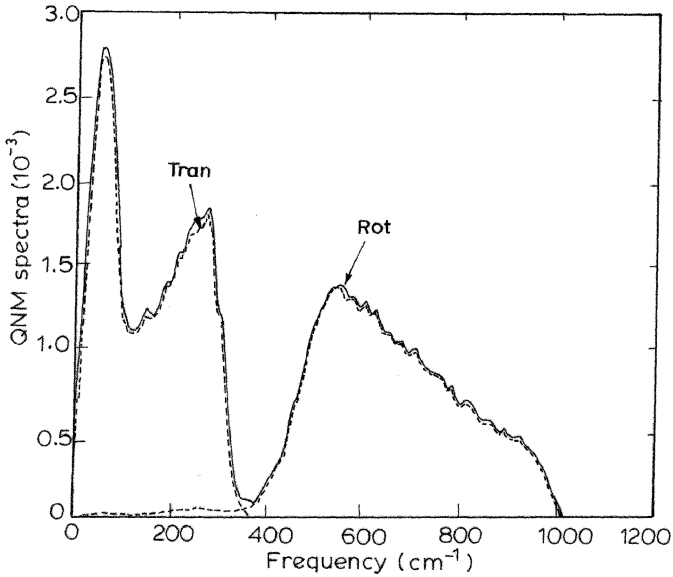

Fig. 1 The partitioning of the quenched normal modes of water into translational and rotational contributions is displayed. The translational (dashed), rotational (dotted), and total (solid) quenched-normal-mode densities of water are shown here. This figure has been drawn with data from reference 74.

band at 50–60 cm^{-1} and a pronounced band around 180 cm^{-1}). The temperature dependence of the spectra gave an activation enthalpy of 2.5 kcal mol^{-1}.[75]

Femtosecond optical Kerr effect (OKE) technique has been used to study low frequency collective dynamics of liquid water, with an aim to disentangle the homogenous and inhomogeneous contributions to the line widths of intermolecular vibrations.[76] If one assumes that the lineshape can be decomposed into a homogeneous part $J(\omega;\Gamma)$ that depends on coupling parameters and inhomogeneous parameters Γ, and an inhomogeneous distribution $\Gamma(\omega)$, then the lineshape can be written as a superposition of the two forms

$$C(\omega) = \int \mathrm{d}\Gamma\, J(\omega;\Gamma)\, \Gamma(\omega) \qquad (1)$$

If one makes the assumption that the polarizability is linear in the normal coordinate Q, then the third order optical response can be expressed directly in terms of $C(\omega)$. By assuming a Brownian oscillator model for the normal modes, one can fit to OHD-RIKE response to obtain the spectral density $C(\omega)$. The $C(\omega)$ obtained by Palese *et al.*[76] at 24 °C is shown in Fig. 2. The study of OHD-RIKES in water gave rise to another interesting result. This is the observation that while OHD-RIKES results are in agreement with dielectric relaxation and NMR studies for "simple" organic liquids,[77] such agreement is lacking with the reorientation rate of water molecules.[78] NMR and dielectric relaxation measurements both give a relaxation time of 8 ps which is more than an order of magnitude larger than the 0.6 ps time observed in the

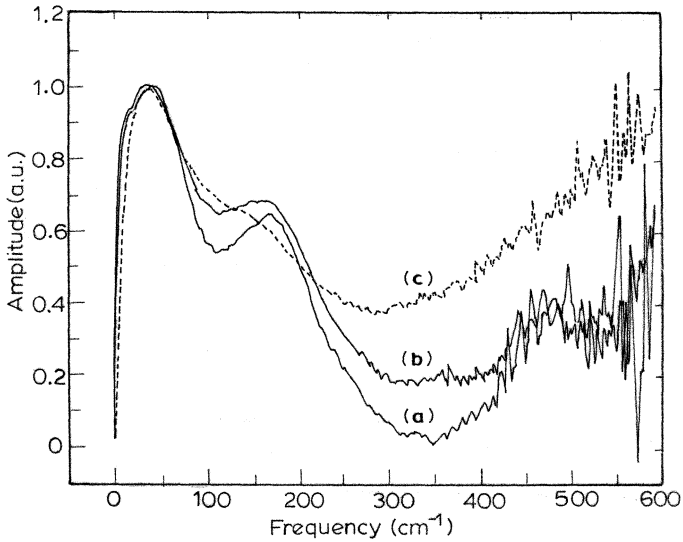

Fig. 2 The temperature dependence of the spectral densities $C(\omega)$ of the OHD-RIKE wave forms and obtained by discrete Fourier-transform analysis premised on the linear coupling hypothesis: (a) corresponds to 2.6 °C, (b) to 24 °C, and (c) to 92 °C. Reprinted with permission from Fig. 3 in reference 79. ©American Chemical Society.

femtosecond OHD-RIKES transient at 24 °C.[79] In addition, the OHD-RIKES signal shows a long lived exponential component which can be explained by the inhomogeneous broadening of the line shape.

2.2 Hydrogen bond lifetime dynamics

The dynamical response of water is intimately connected with the lifetime of hydrogen bonds. The lifetime of a hydrogen bond is usually described in terms of the hydrogen bond lifetime correlation functions,[80–84] denoted by $C_L(t)$ and $S_L(t)$ which are defined by the following expressions:

$$C_L(t) = <h(0)h(t)> \quad (2)$$

$$S_L(t) = <h(0)H(t)> \quad (3)$$

where $h(t)$ is the hydrogen bond lifetime function which is unity if the hydorgen bond between a pair of neighboring water molecules is intact at time t and zero if it is broken, and $H(t)$, on the other hand, is unity only if the tagged bond has remained continuously non-broken from time $t = 0$ to the present time t. Thus, $C_L(t)$ allows hydrogen bonds to be broken and reformed in the time interval t while $S_L(t)$ does not allow such reformation. Both the two functions are found to depend on the criteria of hydrogen bond forming/breaking. However, the numbers from different criteria are

not too different. The lifetime given by $S_L(t)$ is only about 0.5 ps while that given by $C_L(t)$ is about 6.5 ps. The decay of these two functions is shown in Fig. 3. The much longer lifetime given by $C_L(t)$ is due to the relative diffusion of the two pairs and reforming the bond after a sojourn.[80–84] The limitation of $S_L(t)$ is that it does not take into account the reformation of the H-bond immediately after breaking while $C(t)$ may give too long a value of the lifetime. Anyway, it is safe to assume *a lifetime of 1–3 ps for hydrogen bonding in water*. Note that this is close to the orientational correlation time of about 4 ps of individual water molecules. However, polarizability of water molecules can have a significant effect on the hydrogen bond lifetime.[85]

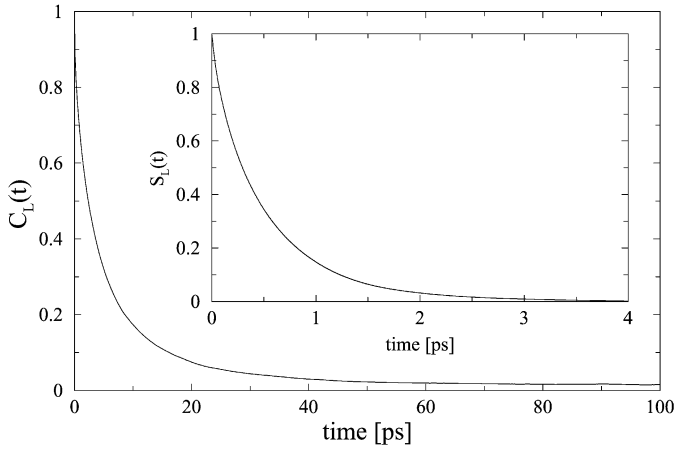

Fig. 3 The time dependence of the hydrogen bond lifetime correlation functions, $S_L(t)$ and $C_L(t)$, defined by eqns. (2) and (3), respectively. Note the much slower decay of $C_L(t)$ than that of $S_L(t)$. This figure has been drawn with data from references 83 and 84.

2.3 Dielectric relaxation

The dielectric relaxation spectrum of pure water has been investigated in considerable detail by different experimental techniques, such as, dielectric loss and more recently, by terahertz technique.[86–93,10] Dielectric relaxation of water has also been investigated by computer simulations. However, the computational efforts have been less successful because of the difficulty of simulating polarizable water. We refer to the Review by Guillot for a recent summary of the computational efforts.[94]

The complex dielectric function, $\varepsilon(\omega)$, can be decomposed into real and imaginary parts

$$\varepsilon(\omega) = \varepsilon'(\omega) - i\varepsilon''(\omega) \tag{4}$$

At room temperature the real part, $\varepsilon'(\omega)$ (the permittivity factor), of pure water is nearly 80 at a few MHz and about 1.8 at 10000 GHz. The imaginary part, $\varepsilon''(\omega)$ corresponds to absorption (dielectric loss) and exhibits a peak at a certain character-

istic frequency ω_m. The dielectric relaxation time, τ_D is equal to $2\pi/\omega_m$. The real and imaginary parts of the frequency dependent dielectric function of pure water are shown in Figs. 4 and 5, respectively.

The dielectric spectrum of pure water in the low frequency region consists of two relaxations with time constants of 8.2 ps and ~1 ps, respectively, with the former one constituting about 90% of the low frequency relaxation. In addition, many high

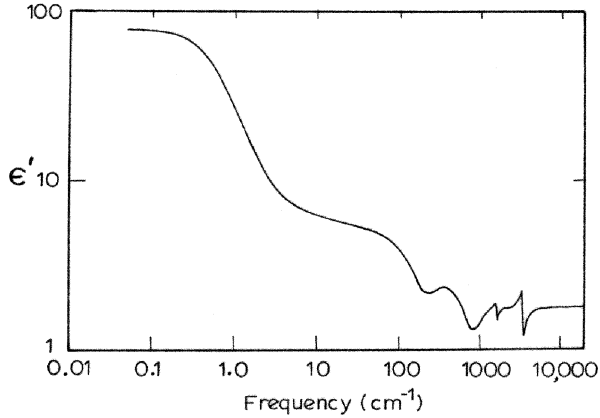

Fig. 4 The real part of the frequency dependent complex permittivity (ε') of pure water at room temperature. Reprinted from Fig. 1 in reference 11, with permission from the the American Chemical Society. ©American Chemical Society.

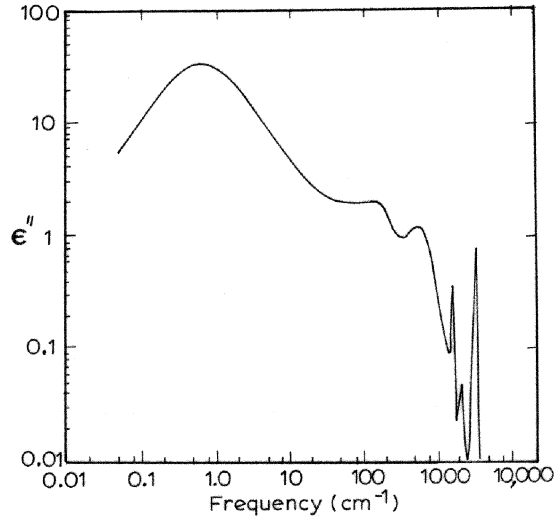

Fig. 5 The imaginary part of the frequency dependent complex permittivity (ε'') of pure water at room temperature. Reprinted from Fig. 2 in reference 11, with permission from the the American Chemical Society. ©American Chemical Society.

frequency modes contribute to the dielectric spectra of water beyond the Debye relaxation regime. As already discussed, this spectral region is extensively investigated by far infrared (FIR) spectroscopic techniques and simulations.[89,90,95–98] In addition to the 200 cm^{-1} band due to the intermolecular O $\cdots$ O stretching and the 650 cm^{-1} band due to libration, there are a few higher frequency bands which are of relatively lesser weight compared to the former two. These high frequency modes are under-damped and, therefore, have different functional forms.[89,99]

2.4 Wave vector and frequency dependent dielectric function of water

Many dynamic processes explore solvent response at small, molecular length scale. Dipolar solvation dynamics contain a significant contribution from nearest neighbour molecules. Electron transfer reactions between two neighboring molecules also involve local dipolar response. Macroscopic dielectric relaxation experiments, on the other hand, provide information only about the long wavelength component of the dipolar response; information about the local response of a dipolar liquid is usually hard to obtain. Theoretically, this information is contained in the wavenumber (k) dependent dielectric function $\varepsilon(k)$ which, at the intermediate wavenumbers ($k\sigma \approx 2\pi$, where σ is the diameter of a solvent molecule), can provide a description of the local polar response. In recent years, several studies have been devoted to the wave vector (k) and frequency (ω) dependence of the longitudinal component of the dielectric function, $\varepsilon_L(k,\omega)$ of water.[100–110] The calculated wave vector dependence of the static dielectric function of water molecules is shown in Fig. 6 where we have plotted the

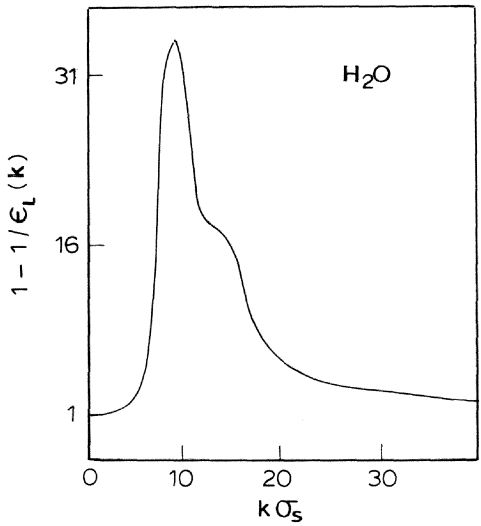

Fig. 6 The wavenumber (k) dependence of dielectric function is diaplayed. Here $1 - (1/\varepsilon_L(k))$ is plotted as a function of $k\sigma_s$ for SPC/E model water at temperature T = 300 K and number density $\rho = 0.033334$ Å^{-3}; σ_s is the molecular diameter of water. The data for this figure are taken from reference 106. Note that in this model, the maximum is at a higher value than $k\sigma_s = 2\pi$.

function $(1 - (1/\varepsilon_L(k)))$: note the sharp maximum of the function near $k\sigma \approx 3\pi$. This maximum shows the existence of strong orientational correlations in water at molecular distances. This is also one of the reasons for the dominance of the first coordination shell in the solvation dynamics of a newly created ion or dipole. Since $(1 - (1/\varepsilon_L(k)))$ is much larger than unity at intermediate values of the wavenumber k, the static dielectric function of water at these values of k is negative! However, this is fully in accord with linear response theory, although it did cause some confusion in the past.[10]

The frequency dependence of $\varepsilon(k,\omega)$ of water is also interesting and the behaviour at intermediate wavenumbers is again dramatically different from that at small wavenumbers.[10] The behaviour at large to intermediate wavenumbers is dominated by the translational diffusion of water molecules. That is, polarization relaxes by diffusion of molecules. This mode of polarization relaxation has been termed "polarization diffusion".[109,110]

3 Overview of experimental studies on aqueous solvation dynamics in the bulk

3.1 Solvation correlation function from time dependent fluorescence Stokes shift (TDFSS) studies

Solvation dynamics has been studied most extensively by monitoring the time dependent fluorescence Stokes shift (TDFSS) of the emission spectrum of a solute probe (typically a dye) whose charge distribution has been changed instantaneously by optical excitation.[3,6,18,42] A very dilute solution of such dye molecules (*e.g.*, Coumarin, Nile Red, Prodan) is usually employed for studying solvation dynamics. These molecules undergo a large change in the dipole moment upon laser excitation, or sometimes may even photo-ionize. Physically, the process of solvation of a solute probe may be described as follows. Consider that a solute chromophore in its ground state is in equilibrium with the surrounding solvent molecules, and the equilibrium charge distribution of the former being instantaneously altered by a radiation field. Ideally, when the solute–solvent system undergoes an optical Franck–Condon transition upon excitation, the equilibrium charge distribution of the solute is instantaneously altered. The solvent molecules still retain their previous spatial and orientational configuration. This is a highly non-equilibrium situation for the system. The energy of the Franck–Condon state is higher than the minimum of the potential energy in the excited state. This is pictorially shown in Fig. 7. Subsequent to the excitation, the solvent molecules rearrange and reorient themselves to stabilize the new charge distribution in the excited state. The final energy is the solvation energy of the solute. The time dependence of the rearrangement of the solvent environment (the 'solvation') is reflected in the continuous red shift of the emission spectrum. The temporal characteristics of solvation is then followed by monitoring the spectral response function (see Fig. 7 for a schematic illustration).

The temporal evolution of solvent is described by the non-equilibrium function $S(t)$, defined by:

$$S(t) = \frac{\nu(t) - \nu(0)}{\nu(0) - \nu(\infty)} \tag{5}$$

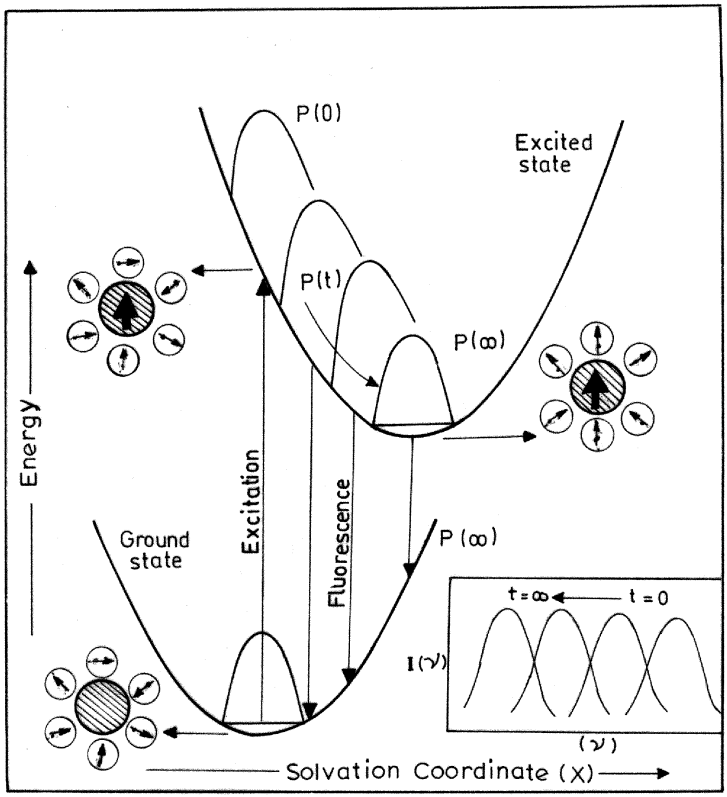

Fig. 7 A schematic illustration of the physical process captured by the time dependent fluorescence Stokes shift (TDFSS). The optical excitation and the fluorescence are shown by arrows. The participating ground and the excited state potential energy surfaces involved in solvation are plotted as a function of the solvation coordinate. TDFSS captures the instantaneous polarization $P(t)$ of the solvent. The inset (bottom right) shows the red shift of the fluorescence spectrum, $I(\nu)$ (ν being the frequency) with time owing to the decrease in the energy of the solute due to progressive solvation.

where $\nu(t)$ is the frequency denoting the position of the emission spectrum whose time dependence describes the red shift of the spectrum of the spectrum subsequent to excitation. Here $\nu(t)$ is determined either by taking the maximum of the spectrum (if the spectrum is symmetric), or by the average over the spectrum, that is $\nu(t) = \int d\nu\ \nu\ I(\nu,t)$, where $I(\nu,t)$ is the time and frequency dependent emission spectrum. $S(t)$, as defined in eqn. (5), varies from unity at time $t = 0$ to zero as time goes to infinity.

The solvation time correlation function is often equated to the auto time correlation function of energy fluctuation. This is usually termed $C(t)$ to distinguish it from $S(t)$. Thus, $C(t)$ is defined as:

$$C(t) = \frac{< \delta E(0)\delta E(t) >}{< \delta E(0)\delta E(0) >} \tag{6}$$

where $\delta E(t)$ is the fluctuation in solvation energy from its equilibrium value at time t. One usually finds $S(t) \approx C(t)$. Therefore, we have made no distinction between the two here.

TDFSS has been applied to a large number of liquids. In an important paper, Jimnez *et al.*[42] reported the results of solvation dynamics of the excited state of dye Coumarin 343. Their result is shown in Fig. 8. The initial part of the solvent response of water is extremely fast (a few tens of femtoseconds) and constitutes more than 60% of the total solvation. The subsequent relaxation occurs in the picosecond time scale.[42] The decay of the solvation time correlation function, $S(t)$, is fitted to a function of the following form:[42]

$$S(t) = A_G \exp(-t^2/\tau_G^2) + B\cos(at)\exp(-t/\tau_1) + C\exp(-t/\tau_2) + D\exp(-t/\tau_3) \quad (7)$$

where, A_G, C and D are the relative weights of the initial Gaussian and the subsequent exponential decay processes and τ_G, τ_2 and τ_3 are the corresponding relaxation time constants. The second term in eqn. (7) takes into account the oscillatory features of the $S(t)$ observed beyond the Gaussian decay in theoretical calculations

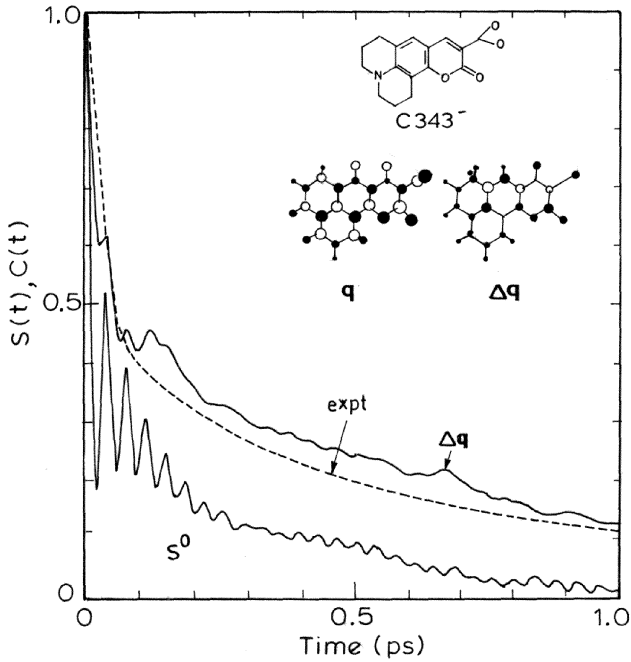

Fig. 8 Experimental (denoted by 'expt.') and simulated (denoted by 'Δq') solvent response functions for C343 in water as obtained by Maroncelli, Fleming and coworkers are shown in this figure. Also shown is a simulation for a neutral atomic solute with the Lennard-Jones parameters of the water oxygen atom (S^0). The experimental data were fitted to eqn. (7) (using the constraint that the long time spectrum match the steady state fluorescence spectrum) as a Gaussian component (frequency 38.5 ps^{-1}, 48% of total amplitude) and a sum of two exponential components: 126 fs (20%) and 880 fs (35%). Reprinted from reference 42 with permission.

and simulations.[42,43,111,112] The early simulation studies also predicted a very fast initial component with a Gaussian time constant less than 10 fs.[111] Fleming and coworkers[42] experimentally detected a Gaussian component of 38.5 ps^{-1} and a slower biexponential decay with time constants 126 fs and 880 fs, respectively. Several other experimental and simulation studies on solvation dynamics of large dye molecules as well as electrons in water demonstrated that the dynamics of solvation in water are indeed ultrafast and occur on the femtosecond scale.[2a,113–127]

More recently, higher order non-linear optical measurements such as three pulse photon echo peak shift (3PEPS) measurements have been carried out to study the solvation dynamics.[128–130]

3.2 Photon echo peak shift spectroscopy

TDFSS is a relatively simple technique use to study solvation dynamics of newly created polar species and has been enormously successful in measuring the solvation dynamics in complex systems. However, this method is not ideal for the study of the initial ultrafast solvation where the dynamics gets convoluted by the instrument response. For example, 55 fs represents the fastest solvation component observed in liquid water by the TDFSS technique. Theoretically, one may expect even faster solvation. The three-pulse photon echo peak shift measurement technique has been developed and applied to study such ultrafast solvation dynamics in bulk water and also in an aqueous solution of protein lysozyme.[62] The key idea of photon echo spectroscopy is based on the fact that subsequent to optical excitation in an inhomogeneous ensemble of absorbers, the transition frequencies in different absorbers become uncorrelated in time. A second pulse is then used to initiate rephasing. If the inhomogeneous width greatly exceeds the homogeneous width, an echo will be produced at a fixed time and the echo will be very narrow in time. We have already discussed that optical and vibrational lineshapes in water are inhomogeneously broadened. Thus, water is an ideal candidate for photon echo studies.

Fleming and coworkers have carried out extensive study of three-pulse photon echo from the dye molecule Eosin in water.[43] They found that a substantial amplitude (about 60%) of aqueous solvation occurs within 30 fs. The observed peak shift is shown in Fig. 9. A three-exponentail fit (up to 100 ps) of Eosin in water data yields time constants 17 fs (73%), 330 fs (15%) and 3 ps (12%). Analysis of the experimental data led Lang *et al.*[43] to attribute this ultrafast solvation to the high frequency intermolecular vibrational/librational modes of water—the hindered translational band at 180 cm^{-1} due to the hydrogen bond network and the 600 cm^{-1} band due to libration. Therefore, the three-pulse photon peak shift provides time constants which are significantly smaller than what could be measured by the TDFSS experiments.

3.3 Red edge excitation shift (REES) spectroscopy

Recently wavelength-selective fluorescence has been used to study solvation dynamics in complex aqueous systems, such as reverse micelles.[131–133] In this method, a shift in the wavelength of the maximum fluorescence emission toward higher wavelength,

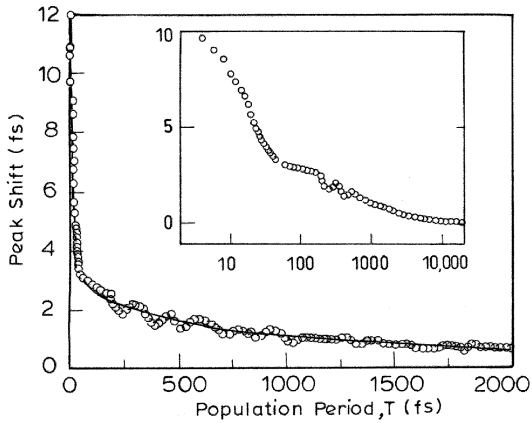

Fig. 9 Three-pulse photon echo peak shift data of Eosin in water (circles) are shown with a simple exponential fit (solid line) as a guide to the eye. The fit includes a ~17 fs (73%) fast component and two slower components, ~400 fs (15%) and ~2.7 ps (12%). The inset, on a log scale and without fit, shows that the peak shift decays to zero by T ~15 ps. Reprinted from Fig. 3 in reference 43, with permission from the the American Chemical Society. ©American Chemical Society.

caused by a shift in excitation wavelength toward the red edge of absorption band, is used to monitor the solvation dynamics. This effect is mostly observed where relaxation is slow so that solvent relaxation is comparable to or slower than the fluorescence lifetime. In a recent study, REES was used to study the rate of solvation in the water pool of reverse micelles. The advantage of REES is that it provides spatial resolution at a molecular level because the fluorescence lifetime is sensitive to the local environment. A drawback of REES is that it is limited by the fluorescence lifetime of the fluorophor, and thus is sensitive to very slow dynamics. In these aspects, REES is similar to NOE.

4 Continuum model predictions

The continuum model of solvation has its origin in the early work of Born and Onsager who derived expressions for solvation energy of polar solutes by modeling the solvent as a homogeneous dielectric continuum and the solute as a sphere with a point charge or point dipole at its center. This continuum model was generalized to treat solvation dynamics by representing the dynamic properties of the solvent through a frequency dependent dielectric constant, $\varepsilon(\omega)$ which is sometimes approximated by the simple Debye formula:

$$\varepsilon(\omega) = \varepsilon_\infty + \frac{\varepsilon_0 - \varepsilon_\infty}{1 + \mathrm{i}\omega\tau_\mathrm{D}} \tag{8}$$

where ε_0 and ε_∞ are the zero and infinite frequency value of the dielectric constant, respectively, and τ_D is the Debye relaxation time. With the above expression for the

dielectric function, the continuum model predicts that solvation dynamics of a newly created ion and of a dipole proceeds exponentially, with time constants given by:[16,17]

$$\tau_L^{ion} = \left(\frac{\varepsilon_\infty}{\varepsilon_0}\right)\tau_D \tag{9}$$

$$\tau_L^{dipole} = \left(\frac{2\varepsilon_\infty + \varepsilon_c}{2\varepsilon_0 + \varepsilon_c}\right)\tau_D \tag{10}$$

where ε_c is the dielectric constant of the solute probe. For water, $\varepsilon_0 = 78.5$, $\varepsilon_\infty = 4.86$. and $\tau_D = 8.3$ ps at 300 K. Thus, the value of the longitudinal relaxation time $\tau_L^{ion} \approx 0.5$ ps. That is, even the continuum model predicts an extremely fast solvation in water! Clearly, the reason for the small value of the predicted solvation time is due to the large value of the static dielectric constant.

Early experimental studies found that while the continuum model prediction of single exponential solvation was incorrect, the *average* time of solvation was rather accurate.[3,18] However, solvation in water turned out to be a different story, as discussed below.

The simple continuum model discussed above has been extended in various directions. Not only a non-spherical shape of the solute but also a space dependence of the dielectric function have been considered.[4] These generalizations lead to somewhat different results, including a non-exponential relaxation of the solvation time correlation function.

In an important recent development, Song and Chandler developed what can be called the ultimate continuum model of solvation dynamics.[134] This theory is based on linear response, uses the full range of frequency dependent dielectric functions and the detailed charge distribution of the chromophore. The predicted solvation time correlation function is in good agreement with the experimental results on aqueous solvation dynamics. This agreement, as discussed later, suggests that at least the initial, ultrafast part of aqueous solvation dynamics is controlled by the *collective* polar response of water.

5 Development of microscopic theories for diffusive solvation dynamics

Strong spatial and orientational correlations present at molecular length scales in liquid water are manifested in the slower part of solvation dynamics. Several molecular theories for polar solvation dynamics were developed to take into account the effects of microscopic structure and some very nice theoretical understanding evolved from them. Early theoretical studies were also motivated by an interesting comment of Onsager[135] who observed that *the polarization structure of water around an electron would form from outside in.* This is the famous *inverse snowball effect*. The inverse snowball picture of Onsager suggests that the relaxation of solvation energy is intrinsically non-exponential since many length dependent time scales are involved.

Onsager's *inverse snowball* model was tested by Calef and Wolynes[136] by using a molecular hydrodynamic theory of solvation dynamics in dipolar liquids. In this approach, the solvation was assumed to be carried out solely by the rotational diffusive motion of the solvent molecules. It was found that Onsager's *inverse snowball* picture was indeed valid in the absence of the translational modes. The calculations of Calef and Wolyness[136] were based on a Smoluchowski–Vlasov equation that was extended to include the translational modes, as discussed later.[137]

Wolynes also extended[138] the linearized equilibrium theories of solvation[139–141] to the time domain. In this approach, the solute was treated as a hard sphere and the solvent molecules as dipolar hard spheres. He showed that if the solvent response is linear to the time dependent variation of the charge distribution on the solute, then the solvation energy relaxation could be described by a bi-exponential relaxation function with one time constant being nearly equal to the longitudinal time constant of the solvent.[138] The second time constant is larger, comparable to the dielectric relaxation time and originates from the slow structural relaxation of the neighboring solvent molecules. Rips *et al.*[142] presented an exact solution of Wolynes's DMSA model for both ion[142a] and dipolar[142b] solvation dynamics.

However, these early treatments did not include the role of solvent translational modes which were included later in a theory where both the rotational and the translational modes of the solvent were incorporated.[10,143,144] The following expression for the longitudinal component of the orientational polarization density relaxation of the solvent has been derived:[137,143]

$$<P_L(-\boldsymbol{k})P_L(-\boldsymbol{k}, t)> = <P_L(-\boldsymbol{k})P_L(-\boldsymbol{k})>\exp(-t/\tau_L(k)) \qquad (11)$$

The equilibrium polarization fluctuation correlation function $<P_L(-\boldsymbol{k})P_L(-\boldsymbol{k})>$ is related to the longitudinal component of the orientational pair correlation function.[10] The longitudinal polarization relaxation time is determined not only by the rotational and translational diffusion coefficients of water but also by the longitudinal component of the two particle direct correlation function $c(110,k)$. The final expression for the time constant is given by:[4,10]

$$\tau_L^{-1}(k) = 2D_R[(1 + p'(k\sigma)^2)(1 - (\rho_0/4\pi)c(110,k))] \qquad (12)$$

where σ is the diameter of a solvent (here water) molecule and $p' = D_T/(2D_R\sigma^2)$. The value of p' determines the relative contribution of the translational modes. A significant contribution from the translational mode could lead to the breakdown of Onsager's conjecture.[135] The importance of the solvent translational mode in the polarization relaxation as found by the above theory is shown in Fig. 10. Note the marked slow down of relaxation at wavenumbers that correspond to nearest neighbour distances ($k \approx 2\pi/\sigma$). This is due to the presence of strong intermolecular orientational correlation among the nearest neighbours. In the opposite limit of small wavenumbers (that is, in the $k \longrightarrow 0$ limit), the above theory reduces exactly to the continuum model discussed above. Note also the small value of the relaxation time at small wavenumbers. There is a nice interpretation for this small value—it is due to the large force constant of the collective longitudinal polarization fluctuation! Thus, the

cause of the ultrafast solvation in water and acetonitrile can be attributed to underdamped solvation in a steep collective polarization potential. The translational contribution is important only at intermediate to large wavenumbers (see Fig. 10). One can easily make an estimate to appreciate the important role of the translational modes. For water, the values of the parameters are as follows: $D_T = 2.5 \times 10^{-5}$ cm^2 s^{-1}, $D_R = 2.2 \times 10^{11}$ s^{-1}, $\sigma = 2.8 \times 10^{-8}$ cm. Thus, for water, the value of the parameter p' is 0.072. When this value is multiplied by $(k\sigma)^2 \approx (2\pi)^2$, we get a value 1.4 which implies that rate of solvation should be approximately 2.4 times faster than the rate given by orientation alone. In the absence of translation, the time constant of the later, slow part of solvation should be in the 4–5 ps range. However, it is predicted to be just about 1 ps. This enhancement of rate is due to the translational motion of the water molecules. While the initial solvation in water is dominated by an ultrafast Gaussian component, translational diffusion is predicted to affect the slower, later part of solvation.

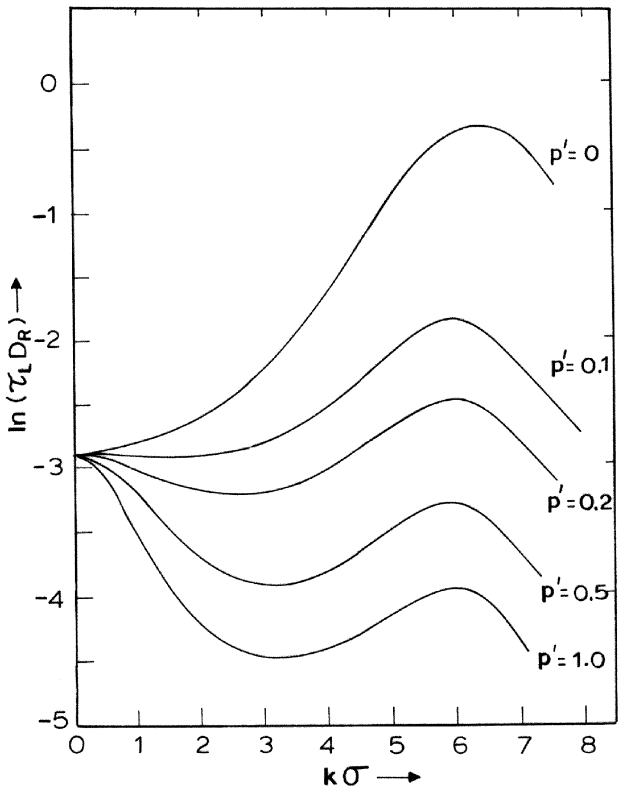

Fig. 10 The dependence of the longitudinal polarization relaxation time on wave vector k and on translational diffusion. The calculated values of $\tau_L(k)$ for several different values of the dimensionless solvent parameter p' ($= D_T/2D_R\sigma^2$). Reprinted from Fig. 1 in reference 142*a*, with permission.

6 Development of microscopic theories for inertial solvation dynamics in water

The molecular hydrodynamic theory[13,99,127,145–147] discussed above has been extended systematically to include the effects of inertial solvent response on solvation dynamics. This approach leads to the following approximate expression for the energy–energy time correlation function, $C_{EE}(t)$:[13]

$$C_{EE}(t) = 4\pi(k_B T)^2 \rho_0 \int_0^\infty dq q^2 S_{ion}(q,t) \mid c_{id}^{110}(q) \mid^2 S_{solv}^{110}(q,t) \tag{13}$$

where $c_{id}^{110}(q)$ is the (110) component of the two particle ion–dipole equilibrium orientational direct correlation function between the ion and a solvent dipole molecule. $S_{ion}(q,t)$ is the self-dynamic structure factor of the ion and $S_{id}^{110}(q,t)$ is the (110) component of the coherent orientational dynamic structure factor of water solvent. The latter is related to the wavevector and frequency dependent dielectric function discussed earlier. The determination of the solvent dynamic structure factor may use the experimental values of the frequency dependent dielectric function: $S(t) = C_{EE}(t)/C_{EE}(t=0)$.

The theoretical results for S(t) are shown in Fig. 11(a) which has been obtained by using *only* the two Debye dispersions. The contributions from the high frequency intermolecular vibration (hydrogen bond excitation) and librational modes are *not* included. As seen here, the decay of the theoretically predicted $S(t)$ is much slower than the experimental results. Fig. 11(b) shows a comparison between theory and experiment when the calculation is done with two Debye *plus* the intermolecular vibration (IMV) and the libration modes. The agreement now is noticeably better. The calculated time constant (after using the two Debye *plus* 193 cm^{-1} IMV band) of the initial decay is faster than the original time constant given by Jiminez *et al.*[42] The lattest 3PEPS measurements[43] show that the initial decay is indeed faster than the original estimate. It has been pointed out by Lang *et al.*[43] that the generalized continuum model theory of Song and Chandler[134] provides a satisfactory description of the experimental data. This may mean that the slower components are more sensitive to the detailed charge distribution of the probe.

The physical picture, which emerged from all the theoretical studies, is shown schematically in Fig. 12. Note the different molecular mechanisms that contribute to different temporal regions.

6.1 Role of intermolecular vibrations (IMV) in solvation dynamics of water: effects of polarizability

The infrared peak near 200 cm^{-1} is related to the interaction induced effects as pointed out by Madden and coworkers[148–150] and is also observed in Raman[151,152] and inelastic neutron scattering[151,153] and is assigned to the O $\cdots$ O stretching mode of the O–H $\cdots$ O unit. This band is located approximately at the same frequency in the

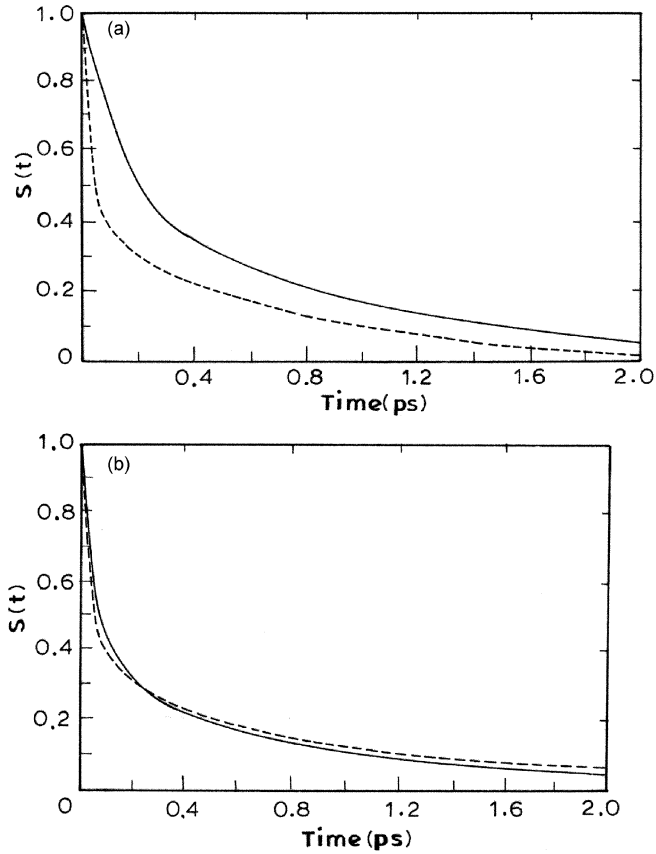

Fig. 11 (a) The prediction of the MHT (solid line) with only two Debye dispersions in the dielectric relaxations is compared to experimental results (dashed line) for the solvation time correlation function $S(t)$. No high frequency contribution to $\varepsilon(z)$ has been included. Reprinted from Fig. 8 in reference 13*a*, with permission. (b) The same comparison as that shown in Fig. 11(a) but with addition of inter-molecular vibrational and the librational contribution. The frequency of the IMV mode is taken to be 193 cm^{-1}, which is responsible for the decrease of the high-frequency dielectric constant $\varepsilon_\infty = 3.48$ to $n_1^2 = 2.1$. The frequency of the librational mode is 685 cm^{-1}, which is responsible for the decrease of the high-frequency dielectric constant $n_1^2 = 2.1$ to $n_2 = 1.77$. Reprinted from Fig. 10 in reference 13*a*, with permission.

Raman and the FIR of H_2O, and D_2O.[154] Since it is due to dipole induced dipole mechanics, this band may be weak or absent in the molecular dynamics simulations[90,155] if the polarizability effects are neglected. Note that simulations do locate a weak Raman peak around 190 cm^{-1}, even when polarizability of the solvent is not taken into account.

If the water molecules were not polarizable, the 200 cm^{-1} IMV would not affect the dielectric relaxation, and, as a result, would not affect the polar solvation dynamics. The IMV and the extended hydrogen bond network would continue to exist even in

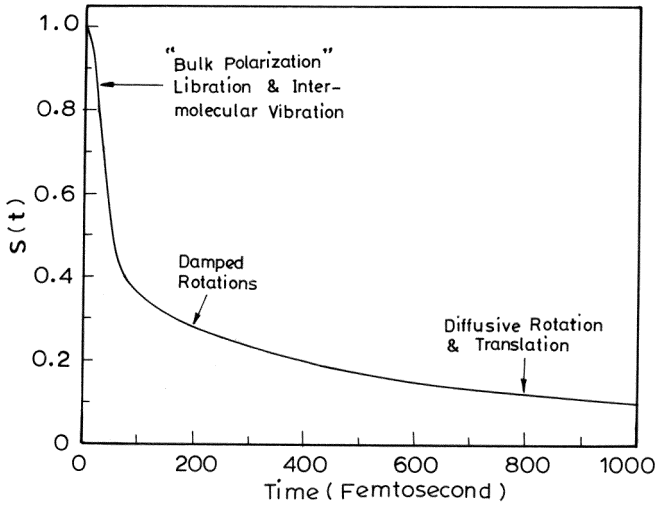

Fig. 12 The theoretical explanation of the physical origin of the three distinct time scales observed in the solvation dynamics in water is indicated clearly on a typical solvation time correlation function. Note that the intermediate ~200 fs time scale is attributed to damped rotation. Reprinted from Fig. 3 (top) in reference 9, with permission from the American Chemical Society. ©American Chemical Society.

the absence of the polarizability. Such a situation indeed arises in computer simulations.[111]

One immediate consequence of neglect of polarizability is that the optical dielectric constant is equal to unity. That is, $n^2 = 1$. Another important consequence is that the dielectric relaxation from $\varepsilon_\infty = 4.93$ to $n^2 = 1$ now must proceed *via* the libration and higher frequency modes. Maroncelli and Fleming performed a detailed simulation study of solvation dynamics in non-polarizable water.[111] Roy and Bagchi[127] have performed a separate set of calculations for $S(t)$ where two Debye dispersion and a single libration (underdamped) are included. The frequency of this libration is taken to be 685 cm^{-1} which is responsible for the dispersion $\varepsilon_\infty = 4.92$ to $n^2 = 1$. The results are shown in Fig. 13 which compare rather well with the simulated results of Maroncelli and Fleming.[114] However, the relaxation rate seems to be faster than what has been observed in experiments,[42] in agreement with theoretical prediction.

6.2 Instantaneous normal mode (INM) approach

In solids, the lattice dynamics is usually described in terms of the normal modes of vibration which are essentially the phonons. On a very short time scale, a dense liquid behaves like a solid and the short time solvent response is essentially elastic. Therefore, it should be possible to construct the phonon picture for classical liquids at short times. In liquids, these modes could be the harmonic oscillation around the equilibrium position of each atom or molecule. This idea of describing liquids at short

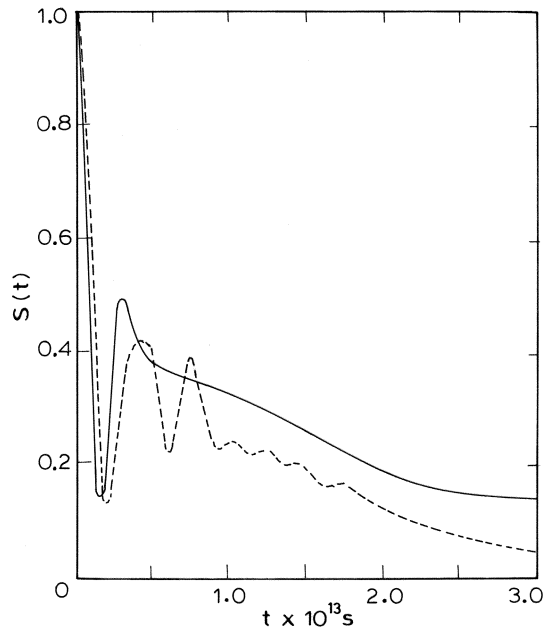

Fig. 13 This figure illustrates the enhancement of the rate of aqueous solvation dynamics when the polarizability of water molecules is ignored (this has been a common assumption of most of the simulations on water). The figure shows the comparison of the calculated (solid line) solvation time correlation function ($S(t)$) with the simulated result (dashed line) of Maroncelli and Fleming.[114] Reprinted from Fig. 2 in reference 127, with permission.

times in terms of elementary excitations (phonon picture) has a long history and has been elegantly described by Zwanzig.[156,157] Since ultrafast solvation occurs on a very short time scale, it is natural that this process can be described by a set of *quasi* normal modes which, even though they have a very short life time (because of mode-mixing), may suffice for this extremely fast relaxation process. A detailed study along these lines has been initiated by Stratt,[158] who coined the term *instantaneous normal modes* for these *transient* modes. Ladanyi, Stratt and coworkers[20,159–164] have carried out a detailed investigation in establishing the mechanism of the ultrafast solvent response at short times. According to the picture provided by Ladanyi and Stratt,[159] the aqueous solvation is dominated by the simultaneous participation of the nearest-neighbor solvent molecules where the solvent libration is the most efficient route to the solvation. This study is also limited by the neglect of the polarizability of water molecules and thus excludes the participation of the inter-molecular vibration in the solvation dynamics.

7 Effects of ultrafast solvation on dynamic processes in water

The discovery that 60–70% of solvation dynamics in water proceeds with a time scale of a few tens of femtoseconds automatically suggests that this can play an important

role in many dynamic processes in water related to solvation. Two such processes are the ion transport in aqueous electrolyte solutions and electron transfer reactions. It is found that in both the cases, ultrafast solvation leads to a dramatic reduction in the polar solvent control of the process. In the following we briefly discuss the new understanding that has emerged due to the presence of the ultrafast component in solvation.

7.1 Ultrafast solvation and ionic mobility in aqueous electrolyte solutions

The limiting ionic conductivity (Λ_0) of small rigid ions, like Li^+, Na^+, K^+, Cs^+, Rb^+, Cl^-, Br^- and others, shows an unusual dependence on the size of the ions. Since the limiting ionic conductivity is proportional to the mobility of the ion, one obtains the following Walden's law by applying the Stokes–Einstein relation between diffusion and viscosity:

$$\Lambda_0 \eta = C/r_{ion} \tag{14}$$

where η is the viscosity of the solvent (here water) and r_{ion} is the crystallographic radius of the ion. The left hand side of the above equation is known as the Walden product. When one plots the Walden product *vs.* $1/r_{ion}$, one obtains a non-monotonic curve with a rather sharp maximum near the cesium ion. This ion size dependence is shown in Fig. 14. The experimental $\Lambda_0\eta$ value for Li^+ is more than an order of magnitude smaller than the prediction of the Walden's law, even Na^+ has a limiting ionic conductivity which is three times smaller than the value given by Walden's law! This unusual behaviour of limiting ionic conductivity in aqueous solutions has drawn the attention of physical chemists for more than a century.

Several theoretical works have earlier addressed the problem on the non-monotonic size dependence of Λ_0.[165–175] The model of Boyd and Zwanzig assumed that the additional friction due to ion-solvent interaction (the dielectric friction) can be calculated by modeling the solvent as a dielectric continuum which is characterized by a Debye dielectric relaxation time τ_D. The prediction of the Zwanzig theory is compared with experimental results in Fig. 14. Note that although the continuum model can capture the non-monotonicity of the limiting ionic conductivity, it vastly overestimates the value of the dielectric friction (that is, underestimates the mobility). The continuum model was further developed by Hubbard and Onsager[167] and the predictions of this theory are also shown in Fig. 14. Although this theory works well for intermediate sized ions, it fails for smaller sizes.

In a marked departure from the continuum model based theories, Wolynes[168,169] developed a molecular theory of ionic mobility by using a molecular hydrodynamic approach where the dielectric friction on the ion was calculated by using the well-known Kirkwood formula[170] which expresses the friction as a time integral over the force-force time correlation function. The latter can be related to the longitudinal polarization relaxation time correlation function. Colonomos and Wolynes[171] performed a numerical calculation of the dielectric friction and obtained good agreement, although the solvent was approximated to have only the Debye dielectric relaxation time—that is, the ultrafast solvation components were not included! In

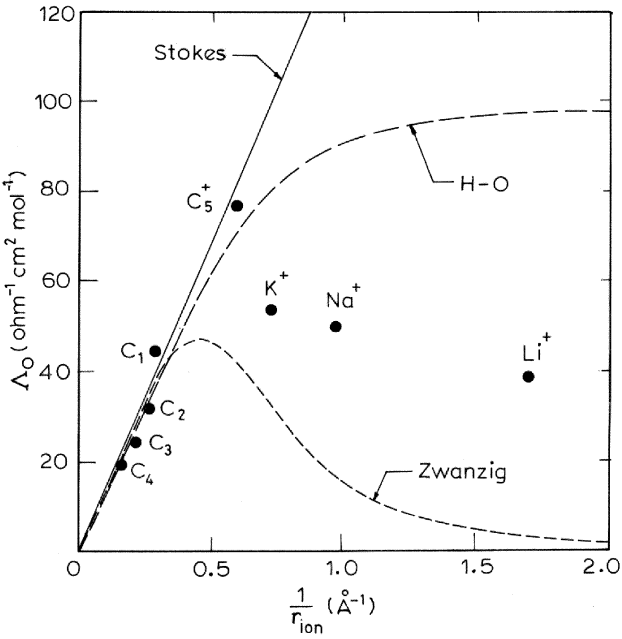

Fig. 14 Comparison of the experimental results on limiting ionic conductivity (Λ_0) with the predictions from the well-known continuum theories. The experimental values of the limiting ionic mobility of rigid, monopositive ions in water at 298 K are plotted as a function of the inverse of the crystallographic ionic radius r_{ion}^{-1}. The experimental results are denoted by the solid circles. The solid line represents the predictions of Stokes's law with a slip boundary condition, the large dashed line represents the Hubbard–Onsager theory, and the small dashed line is the prediction of the theory of Zwanzig with a slip boundary condition. Note that Stokes's law is quite valid for the large tetra-alkyl ammonium ions. Reprinted from Fig. 2 in reference 13*b*, with permission from the the American Chemical Society. ©American Chemical Society.

order to remove this lacuna, recently a detailed microscopic theory has been developed which includes not only the effects of ultrafast solvent modes but also a detailed intermolecular spatial and orientational correlation function. The predictions of this theory are in reasonable agreement with the experimental results, as shown in Fig. 15. It was further found that the *ultrafast solvation modes play an important role by significantly lowering the value of the dielectric friction by opening up fast relaxation channels of the fluctuating force–time correlation function*. If one includes only the slow (10 ps) component of polarization relaxation, then the theory predicts mobility that is comparable to Zwanzig's continuum model.

There have been several computer simulation studies of ionic mobility in water, Berkowitz and Wan[176] have examined the assumption made in analytical theories concerning the cross-correlation between the spherical, non-polar part of the interaction potential and the angular ion–dipole interaction. Neglect of this cross-correlation allows one to write the total friction as a sum of Stokes friction due to viscosity and the dielectric friction due to polar interactions. Simulations of Berkowitz and coworkers show that such a separation could be questionable.[177] Lee and

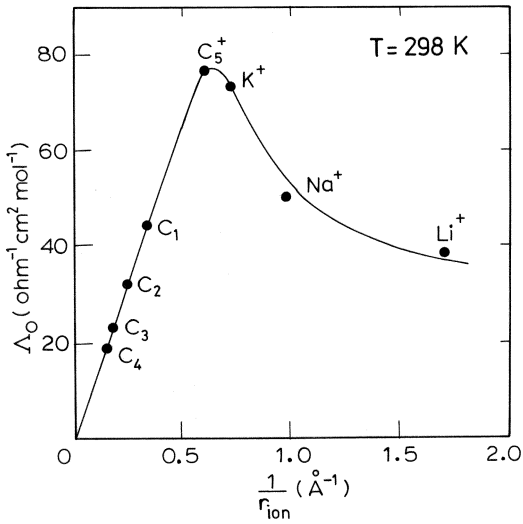

Fig. 15 Comparison of the values of the limiting ionic conductivity Λ_0 of rigid, monopositive ions with the prediction of the molecular theory that takes into account of the ultrafast sub-50 fs solvation dynamics in liquid water. Here Λ_0 is plotted as a function of the inverse ionic radius r_{ion}^{-1} in water at 298 K. The solid line represents the predictions of the microscopic theory. The solid circles denote the experimental results. Reprinted from Fig. 4 in reference 13*b*, with permission from the American Chemical Society. ©American Chemical Society.

Rasaiah[178] carried out extensive molecular dynamics simulations of ionic mobilities of both anions and cations, by taking into account the differing interaction potential of these two ions with water. These simulations could reproduce semi-quantitatively the difference in ionic mobility between halide anions and alkali cations—experimentally these two series fall on two different curves, although the sizes are comparable. The theories of dielectric friction have not yet been extended to address this difference. An interesting outcome of the simulations of Lee and Rasiah[178] is the marked dependence of the conductivity on the ion–solvent and solvent–solvent interaction potential.

7.2 Dynamic solvent effects on electron transfer reactions

As the motion of an electron can be strongly coupled to solvent polarization modes, the dynamics of solvent polarization can in principle have complex and diverse effects on the rate of an electron transfer.[179–184] However, the extent of these solvent effects is largely determined by the electronic coupling between the two participating potential energy surfaces. Thus, solvent effects are expected to be minimal for non-adiabatic electron transfer reactions where the electronic coupling between the two surfaces is small and the rate is determined by this coupling. In the opposite limit of an adiabatic electron transfer reaction when the coupling is so strong that ETR occurs on a single ground state potential energy surface, solvent effects can be very important. It was

pointed out by Zusman [180] that in this limit, the electron transfer rate could be determined by solvent fluctuations. The Zusman expression for the rate is given by: [180]

$$k_{et} = \frac{1}{\tau_L^{ion}} \exp(-E_a / k_B T) \tag{15}$$

where E_a is the activation energy of an adiabatic electron transfer reaction, given by the well-known Marcus expression and τ_L^{ion} is the longitudinal relaxation time, given earlier by eqn. (11). In a seminal paper, Hynes [181] extended Zusman's theory [180] to treat non-Debye solvent relaxation and showed how to link solvent effects directly to the solvation time correlation function. In essence, the theory uses Grote–Hynes [182] theory to calculate the rate of an adiabatic electron transfer where the frequency dependent friction is obtained from solvent time correlation functions. In Fig. 16, the real part of the friction on the electron transfer reaction is shown, as obtained by using the solvation time correlation function in water, acetonitrile and methanol. The friction has been scaled by the zero frequency friction in each case. Note that if ultrafast solvation is neglected, then the friction on the reaction motion is equal to the zero frequency friction in each case. In that limit, we get back Zusman's result. However, *due to the*

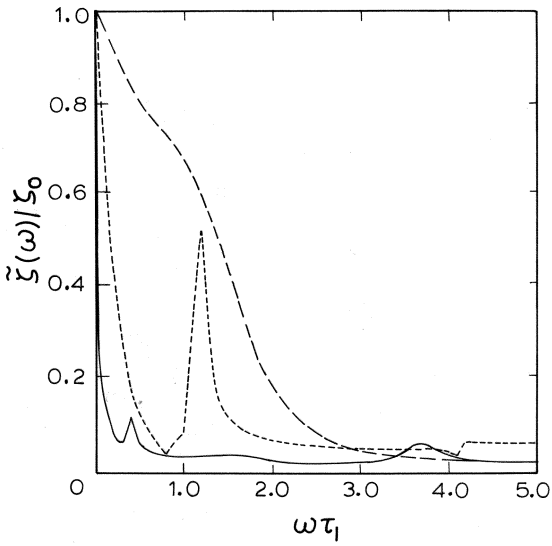

Fig. 16 The real part of the frequency dependent friction, $\tilde{\zeta}(\omega)$, acting along the reaction coordinate for an adiabatic electron transfer reaction, is plotted as a function of the Laplace–Fourier frequency, ω, for an outer-sphere electron transfer reaction in methanol (solid line), water (short dashed line) and acetonitrile (long dashed line). ζ_0 Is the zero frequency friction of the respective solvent. $\zeta_0 = 6.18 \times 10^{15}$ s^{-1} for methanol, 1.05×10^{15} s^{-1} for water and 2.54×10^{13} s^{-1} for acetonitrile. The frequency is scaled by τ_1 which is equal to 0.06, 0.1 and 0.45 ps for methanol, water and acetonitrile, respectively. The solute to solvent size ratio is 3.0 in all the three solvents. Reprinted from reference 127*b*, Fig. 2, with permission from the American Chemical Society. ©American Chemical Society.

presence of the ultrafast solvent modes, the friction on the reaction is much reduced. The results are particularly striking for water. If ultrafast solvent modes are neglected, then the rate of an adiabatic electron transfer reaction is predicted to be strongly reduced, even for a weakly adiabatic reaction, in contradiction to the experimental results. The ultrafast solvent modes drastically reduce the friction at the reactive frequency and as a result, weakly adiabatic reactions are predicted to obey the transition state theory. Actually, some of the above results were found *via* simulations by Carter and Hynes.[184] However, the origin of the absence of solvent effects was fully understood only after the sub-100 fs ultrafast solvation in water was discovered.

8 Water solvation dynamics in several related systems

In the following we discuss recent developments in several important related areas where studies on solvation dynamics were motivated by the new results obtained in bulk water. The coverage is not exhaustive but aims at providing a glimpse of these emerging areas.

8.1 Dynamics of solvation in aqueous electrolyte solutions

Huppert *et al.*[185] and Chapman and Maroncelli[186] carried out experimental studies of solvation dynamics in aqueous electrolyte solutions of varying ion concentration ranging from 10^{-3} to 3 M. It was found that the relaxation of the ion–solution interaction energy can be separated into its solvent and ionic components. The solvent response was found to be much faster than the ionic relaxation. An interesting observation of these studies is an increase in the long-time solvation rate with an increase in the ion concentration. This effect is rather strong, as shown in Fig. 17. Neria and

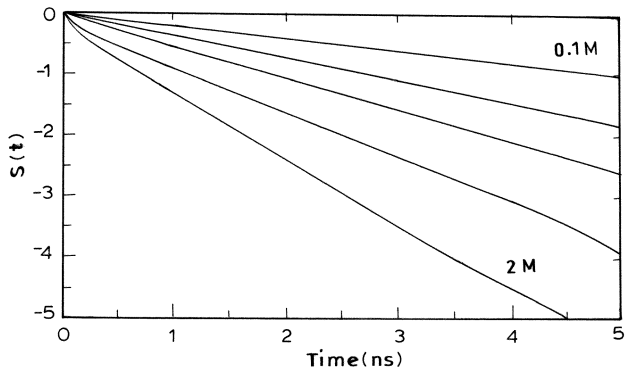

Fig. 17 The time dependence of the spectral response functions, $C(t)$, of Coumarin 102 in $NaClO_4$/acetonitrile solutions at various salt concentrations. From bottom to top the salt concentrations are 0.1, 0.25, 0.5, 1.0 and 2.0 M. Reprinted from Fig. 7(b) of reference 186, with permission from the American Chemical Society. ©American Chemical Society.

Nitzan[187] have carried out a detailed computer simulation study of solvation dynamics in ionic solutions. They found that there is a fast Gaussian decay characterized by the Gaussian time constant τ_G which is followed by a very slow exponential-like decay. It was also found that the Gaussian time constant is practically independent of ion concentration whereas the long exponential time constant depends rather strongly on ion concentration and it decreases when the ion concentration is increased. On the theoretical side, van der Zwan and Hynes[188] studied the role of the ion atmosphere relaxation on dipole solvation dynamics by employing a primitive model of the solution and the Debye–Falkenhagen theory[189] of ion atmosphere relaxation. Because of the use of a primitive model, the effects of solvent dynamics could be considered in their theory.

Recently, Chandra and coworkers[190–192] presented a molecular theory of ion solvation dynamics in aqueous electrolyte solutions, which properly includes the molecularity of both solvent and ions. In their study, a fast initial decay was found in the solvation dynamics which was then followed by a slow exponential decay, in agreement with the observations of experiments and computer simulations.[190–192] According to this theory, at short times the relaxation of $S(t)$ is Gaussian with a time constant which is essentially the same as in bulk water. The long decay is predicted to be exponential with a time constant t_M which is inversely proportional to the conductivity σ of the solution. Thus, while the initial Gaussian decay depends only *weakly* on ion concentration, the long time decay of the solvation time correlation function decreases with ion concentration. Thus, the predicted ion concentration dependence of solvation dynamics is consistent with the experimental results of solvation dynamics in solutions of varying ionic strength (Fig. 17).

8.2 Dynamics of electron solvation in water

The quantum nature of the electron, its light mass and high polarizability, coupled with the large polarizability of oxygen and the hydrogen bond network of water, make the issue of solvation dynamics of electrons in water unconventional. Many experimental, computer simulation and theoretical studies have been carried out to understand this interesting problem which has relevance to reactions in water. Initial femtosecond spectroscopic studies of Eisnethal and coworkers[193] and Gauduel *et al.*[194,195] showed that before the electron gets solvated, it takes about 100 fs to get localized. Computer simulations of Schwartz and Rossky[196] found the solvent response function to be bimodal with an initial Gaussian component of about 25 fs. The rest of the solvation is relatively slow with a time constant of 250 fs. Barbara and coworkers[197] studied the solvation dynamics of hydrated electrons in water by using femtosecond pump–probe spectroscopy, with 35 fs resolution. They measured the signal at different wavelengths both for normal and heavy water. This experimental study confirmed many of the predictions made by earlier workers.[123,196,198] The observed dynamics primarily reflected the p-state solvation with a time constant of initial ultrafast inertial solvation in the 30–80 fs range. Thus, the current understanding of the physical process involved in electron solvation appears to be as follows. At first the excited electron undergoes displacements in the search for a pre-existing trap. This search is accompanied and facilitated by the orientational polarization of the water molecules away

from the electron. This collective polarization gives rise to a spectral shift in the 30–80 fs range, just as in the case of an ion in bulk water. This leads to the formation of an equilibrated and solvated p-state electron. The non-adiabatic transition to the s state occurs on a much slower time scale. The solvation of the newly created s-state is again fast, occurring in the sub-100 fs time scale. On the theory side, Rips[114–116] has presented a hydrodynamic model of electron solvation where the solvation process is assumed to involve a contraction of the initial cavity size.

8.3 Solvation dynamics in supercritical water

The critical point of water is located at a pressure (P_c) of 22.1 MPa, temperature (T_c) of 847 K and density (ρ_c) of 0.32 g cm^{-3}. By supercritical water (SCW) one usually means water at high temperature (above 847 K) and relatively high density. At such a high temperature, the extended hydrogen bond network of liquid water becomes essentially non-existent and water shows certain remarkable properties. The dielectric constant of SCW is only 6, making it similar to organic solvents in many respects.[199] Thus, many organic solutes, like benzene and toluene are soluble in SCW which makes it a suitable future material for extraction and cleaning processes. Simulation studies of solvation dynamics in SCW have been reported for the first time by Re and Laria.[200] Their studies indicated a biphasic decay of solvation energy, with an ultrafast decay, rather similar to that observed for bulk water. This is rather surprising because here the density is low, the extended hydrogen bond network is non-existent, thereby eliminating contributions from the libration and the intermolecular vibration modes. Their results were subsequently corroborated by theory[201] which shows that the ultrafast component arises here from the very fast rotational motion of small water molecules. These results are yet to be verified experimentally. Recent simulation studies[202,203] find that the solvation dynamics in SC CHF_3 and CO_2 is biphasic in nature. The fast component of the total solvation energy here decays with a time constant of about a picosecond. The other component relaxes at a rate with a time constant in the tens of picoseconds regime. A set of very recent experimental studies[203] employing the time correlated single photon counting technique has, however, indicated that the slow component has a time constant of about 50–70 ps which is much slower than that observed in the above simulation.

9 Water dynamics in protein hydration layers

As already mentioned, the water molecules in the immediate vicinity of biomolecules (proteins and DNA) and complex systems (micelles, lipids) exhibit dynamic properties that are quite different from those in the bulk.[21–31] In these systems, water molecules experience a surface that is heterogeneous, even on a molecular length scale and the interaction with the surface is often quite strong, leading to a disruption of the hydrogen bond network of bulk water. Measurements of the rotation and translation diffusion coefficients of proteins in aqueous protein solutions show that an explanation of the observed values requires that a radius, larger than the actual radius, of the protein be used in the Stokes expression of the friction (from hydrodynamics).[22,23] The study

of the nuclear Overhauser effect (NOE), gave an upper limit of 500 ps of residence time for most of the water molecules in the layer.[30] Other sources of information about biological water are from X-ray diffraction and neutron scattering.[204,205] Both give, in the crystalline form of the protein, a measure of the number of bound water molecules. Typically, 60–70% of the exposed sites of a protein are found, on the average, to be occupied by water molecules. Recent computer simulations and solvation dynamics experiments provide detailed information about the dynamics of biological water.

9.1 Computer simulation studies of hydration dynamics

In the following, we summarize some of the results obtained by molecular dynamics simulations of hydration water. (i) The residence time of water molecules in the hydration layer of myoglobin is found to have a distribution between somewhat less than 30 ps to more than 80 ps which was the longest run time of the simulation[204,205] The water molecules with much longer residence times are those which are either buried inside protein cavities or in the clefts or have multiple interactions with the protein and have higher (than average) binding energies. The binding energy distribution has values ranging from 0.5 to 9 kcal mol^{-1}. (ii) Gu and Shoenborn found a strong peak in the radial distribution function for hydrogen bonding between the protein surface and water molecules.[205] (iii) The trajectory of individual water molecules clearly shows two entirely different behaviours—one for the bound state and the other for the moving (free) state. Rapid exchange between the two states was observed suggesting the *existence of a dynamic equilibrium between the two states*.[204,205] (iv) Simulations suggest a lower number of tightly bound water molecules than observed in diffraction measurements. In a study of the dynamics of the protein hydration layer, Rocchi *et al.* calculated a layer survival correlation time which was allowed to decay when a water molecule leaves or enters the layer.[206] This correlation function was found to decay slowly for the nearest layer. (v) The average orientational time correlation function was markedly non-exponential and the average translational motion was sub-diffusive. The orientational time correlation function can be fitted to a stretched exponential with the value of the exponent significantly less than unity. Marchi *et al.* found that the rotational relaxation of water in the vicinity of a simulated lysozyme is 3–7 times slower than that in the bulk, depending on how the hydration shell is defined.[207] The same simulation also reported the observation of the sub-diffusive diffusion of water molecules. (vi) A recent simulation study of the hydration of protein ribonuclease A reported that at room temperature and at high hydration, significant translational and rotational motions occur.[208] (vii) Boresch, Hoechtl and Steinhauser have simulated the frequency dependent dielectric properties of ubiquitin solution by a long MD simulation.[209] They observed a significant dielectric increment for the static dielectric constant at low frequencies but a decrement at high frequencies (which is of course expected). When the overall dielectric response was decomposed into the protein–protein, water–water and the water–protein cross terms, the most important contribution was found to arise from the self-term of water. Simulation beautifully captured the bimodal shape of the dielectric response function as has often been observed in experiments. This is shown in Fig. 18,

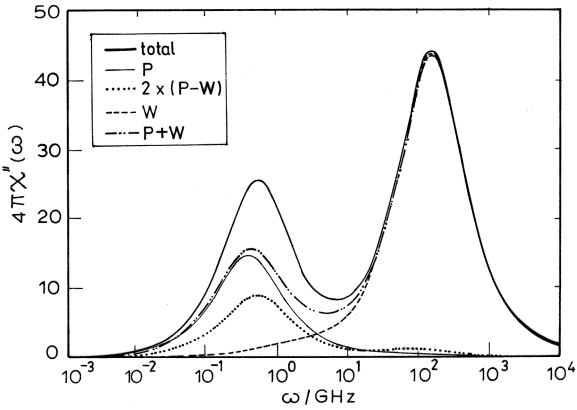

Fig. 18 The simulated frequency-dependent dielectric loss $4\pi\chi''(\omega)$ of the components of a 0.0093 M aqueous ubiquitin solution: protein–protein (P) and water–water (W) self-terms, as well as 2 the protein–water cross-term (P–W). In addition, $4\pi\chi''(\omega)$ of the solution as a whole (total) and the sum of the protein and water self-term, *i.e.*, the overall spectrum minus the protein–water cross-term, is given (P + W). Reprinted from Fig. 4 in reference 209, with permission from the American Chemical Society. ©American Chemical Society.

where the relative contributions of the pure and cross-terms, as found by Boresch *et al.*,[209] are also indicated. Pettitt and coworkers[26] have presented an elegant physical picture of solvation and hydration of proteins and nucleic acids, based on extensive computer simulations and theoretical calculations.

9.2 Dielectric relaxation of aqueous protein solutions

The dielectric spectra of aqueous protein solutions have been a subject of long standing interest and have been reviewed recently.[11] These solutions exhibit an anomalous dielectric increment.[210,211] A typical experimental result illustrating the dielectric increment is shown in Fig. 19 where the real part of the frequency dependent dielectric constant of myoglobin is evident. Not only the increment, but the shape of this curve also, has drawn a lot of attention. In a detailed review, Oncley[212] discussed the effect of orientational motions of the large protein molecules and smaller water molecules on the dielectric spectrum of an aqueous protein solution and proposed that the dielectric increment arises solely due to the contributions of the protein molecules. According to Kirkwood and Shumaker,[213] the fluctuation of the dipole moment due to proton transfer could be responsible for the observed low-frequency dispersion. In an important departure from the above physical models, Jacobson[214] proposed a model of structured water surrounding the macromolecule to explain the dielectric properties of aqueous protein solutions. Most recently inelastic incoherent neutron scattering data support the existence of structured water around proteins.[215]

There are certain universal features in the dielectric relaxation spectra of aqueous protein solutions. One usually finds two distinct loss peaks near 10 MHz and 10 GHz.[216,217] These two peaks correspond to the protein and bulk water relaxations,

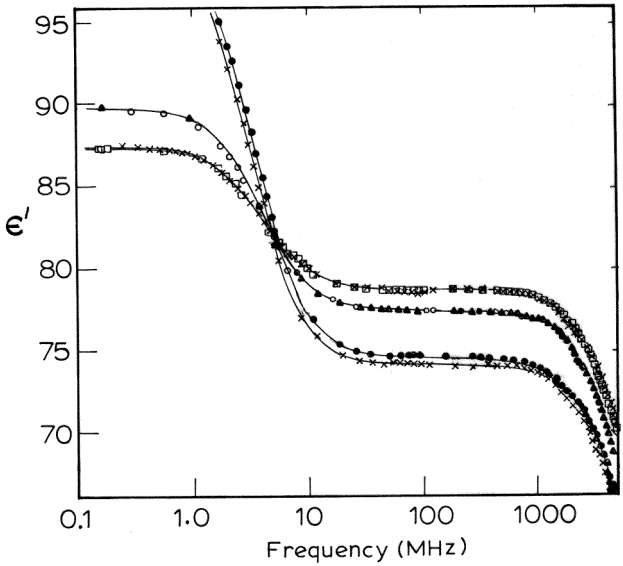

Fig. 19 Concentration dependence of the real part of the complex frequency-dependent dielectric function (ε') of aqueous myoglobin solution (concentrations are 77, 99 and 161 mg mL^{-1}, respectively) as obtained from different experiments at 293.15 K. The symbols denote experimental results[11] while the solid line is a fit to the theory of Nandi and Bagchi.[21] Plots of different concentrations as obtained from the theory and experiment are indicated by different symbols. Reprinted from Fig. 11 of reference 11, with permission from the American Chemical Society. ©American Chemical Society.

respectively (see Fig. 18). The additional high frequency dispersions, observed within the range of 10 MHz to 10 GHz, are often referred to as δ dispersion (δ_{11} and δ_{22} dispersions). While the two peaks near 10 MHz and 10 GHz are high and distinct, the dispersion occurs in the plateau region of the dielectric spectra and has relatively less weight.[217] Dachwitz *et al.* suggested that the dispersion is due to the *bound water* and internal motions of myoglobin.[216] Similar results were obtained for other proteins.[217] Mashimo *et al.* assigned the low frequency process to the relaxation of bound water and the high frequency process to the relaxation of free water, respectively.[218]

The almost universally observed bimodal relaxation dynamics of water near a biomolecule have been explained recently by Nandi and Bagchi[21] in terms of a dynamic exchange model between the free and bound water states. Halle and cowokers[219,220] suggested a similar dynamic exchange between the slowly rotating internal and the fast external water molecules from the NMR relaxation of ^{17}O nuclei.

9.3 Experimental studies on solvation in the hydration layer

Several important solvation dynamics experiments have been carried out very recently on the solvation dynamics of probes at hydrated protein surfaces and reported that the solvation dynamics of protein bound fluorophores is significantly

slower compared to that in bulk water. Pierce and Boxer[221] and Bashkin *et al.*[222] reported that the solvation dynamics in the protein environments is non-exponential with a long component with a time constant of the order of 10 ns. It is interesting to note that this time scale is very close to the nanosecond component of the dielectric relaxation earlier observed for the aqueous protein solutions.[21,211] Fleming and coworkers used the three-pulse photon echo peak shift technique to examine the solvation of Eosin at the surface of aqueous lysozyme.[62] In addition to the ultrafast bulk water response discussed earlier, they found a slow component which is as slow as 500 ps. This slow component was found to have an amplitude of 8%. The experimental result of the solvation–time correlation function of Eosin in lysozyme is shown in Fig. 20. Analysis of the experimental data *via* the generalized continuum model of Song and Marcus led to the conclusion that the slow component originates from the motion of the side-chains of the protein.

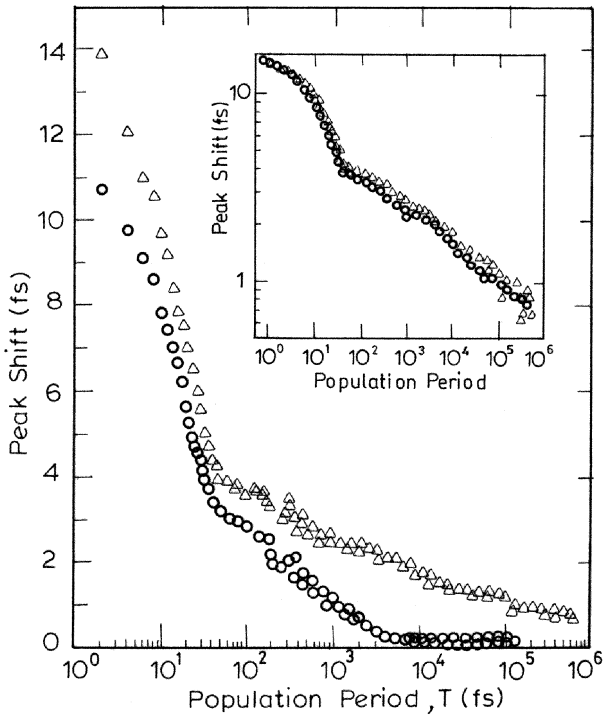

Fig. 20 Logarithmic (log) plot of the peak shift data of Eosin in water (solid circles) and lysozyme complex in water (open triangles). The inset shows a log–log plot of the lysozyme data (open triangles) with fit (solid line). Reprinted from Fig. 4 in reference 62, with permission from the American Chemical Society. ©American Chemical Society.

In a series of elegant experiments,[9,65] Zewail and coworkers have examined the solvation dynamics of newly excited tryptophan in several proteins. The advantage of using tryptophan as a probe is two-fold. First, it is a natural probe, so conformation

of the protein is not disturbed and solvation of the native state is explored. Second, one can study proteins where the tryptophan is partly or fully exposed to water, and so solvation dynamics studies allow one to probe the response of biological water. Zewail and coworkers found a slow component in the solvation time correlation function which is in the range of 20–40 ps.[9,65] This is more than an order of magnitude slower than the bulk response. The results of Zewail and coworkers are shown in Fig. 21 for the protein Subtilisin Carlsberg (SC). The inset in the same figure shows the faster solvation when the probe is dansyl bonded and placed at a distance of 6–7 Å from the protein surface. The results of these studies have been interpreted by using the dynamic exchange model discussed below.

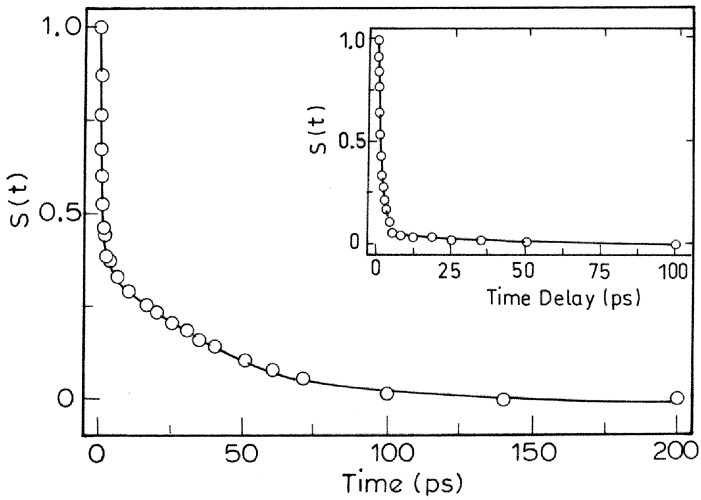

Fig. 21 Experimental determination of the hydration time correlation function for tryptophan probe in the surface of the protein Subtilisin Carlsberg (SC). The inset shows the same for Dansyl bonded SC where the probe is 6–7 Å away from the surface. Reprinted from reference 9 with permission from the American Chemical Society. ©American Chemical Society.

9.4 Quantitative predictions of the dynamic exchange model

The dynamic exchange model[21,9,31b,219,220] envisages the emergence of multiple (especially slow) time scales due to the existence of a dynamic equilibrium between the bound and free water molecules in the surface of biomolecules or self-assembly. At the centre of this model lies the assumption that the water molecules at the surface of proteins can be considered as distinct species because of their strong hydrogen bonding to the biomolecular surface. This equilibrium can be symbolically written as:[21,31b]

$$\text{bound water} \Leftrightarrow \text{free water}$$

Bound water is not a unique species because there is a distribution of the energies of binding of water molecules to the protein surface. This distribution, denoted by $P(\varepsilon)$, is rather interesting. Simulations suggest an exponential distribution of the residence

time, with a very sharp fall at low values of ε. A schematic illustration of the energy distribution is shown in Fig. 22—the low values of ε correspond to quasi-free water molecules near the hydrophobic surface. The bound water molecules are expected to have a broad distribution centred around a relatively large binding energy. An estimate of the new time scale due to this dynamic exchange can be obtained as follows. If $V_i(z)$ denotes the reduced energy of interaction of a water molecule with the site i on the protein surface (here z is the direction perpendicular to the surface), $V_i(z)$ will have a minimum at $z \sim 3$–3.5 Å. At smaller distances from the surface, the energy rises sharply. The potential is shown schematically in the inset of Fig. 22 where all of the coordinates are also shown.

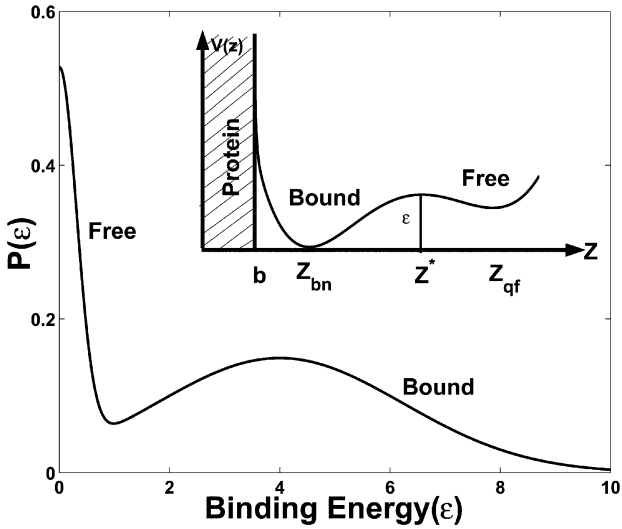

Fig. 22 A schematic illustration of the probability density function, $P(\varepsilon)$, of the binding energy, ε, of water molecules on a protein surface. The first peak at zero binding energy corresponds to the quasi-free water molecules while the broad maximum at a larger value corresponds to the transiently bound water molecules to sites of large binding energies (*e.g.* arginine). The inset shows a schematic illustration of the potential energy surface $V(z)$ that a water molecule experiences near the protein surface. The Z-direction indicates the distance from the protein surface. $Z = b$ denotes a position at the surface where the potential energy becomes much larger than the thermal energy, k_BT. The reflective barrier in the mean first passage time calculation is placed at this position by the method of images. $Z = Z_{bn}$ denotes the average position of the bound state and $Z = Z_{qf}$ that of the quasi-free state. Z^* indicates the position for the activation barrier.

9.5 Orientational and dielectric relaxation

An expression for this slow relaxation has been derived by using the dynamic exchange model. The starting point is the coupled reaction–diffusion equations of Nandi and Bagchi,[21] which can be solved to obtain the two rate constants, $k_{\pm}$, for the dipolar orientational correlation function. These rates are given by:[9]

$$k_{\pm} = 0.5[-B \pm \sqrt{(B^2 - 4D_R k_{fb})}] \qquad (16)$$

with $B = 2D_R + k_{bf} + k_{fb}$, where D_R is the rotational diffusion coefficient of the free water molecules, k_{bf} is the rate of the free to bound transition and k_{fb} is the rate constant of the reverse process. Typically, the rate constant of the free to bound reaction, k_{bf}, will be larger than that for the reverse process, k_{fb}. In the limit when the rate of conversion from bound to free becomes very small, the above expression further simplifies and the two rate constants are given by $2D_R$ and k_{fb}. Thus, while one time constant remains fast, of the order of 4–5 ps, the other is predicted to slow down appreciably, even to the extent of hundreds of picosecond. The rate constant k_{fb} is of course determined by the binding energy. For the majority of sites, the time constant may range between 20 and 500 ps or so.

9.6 Theory of slow solvation dynamics in the hydration shell

Solvation dynamics of a probe located at the surface of a protein is rather complex because the probe derives contributions from three different regions: (i) the host protein molecule, (ii) the water in the hydration shell, and (iii) the bulk water. Experiments have shown that even in this case the ultrafast sub-100 fs component continues to exist[62] and it is likely that the origin of the ultrafast component remains the same[43] *i.e.*, the collective polarization relaxation of bulk water molecules. The sub-200 fs decay can, in principle, derive contributions from high frequency protein motions. The new element is the emergence of a slower component with a time constant in the range 20–500 ps, depending on the protein studied.

The dynamic exchange model predicts the two wavenumber (k)-dependent relaxation times limiting time constants to be given by:[9]

$$\tau_{fast} \approx \tau_s^{bulk} \tag{17a}$$

$$\tau_{slow} \approx k_{fb}^{-1} \tag{17b}$$

In the same limit of large activation energies separating the bound state from the free one, the residence time of the bound water molecules is given essentially by k_{fb}^{-1}. This also gives the residence time of strongly bound water. This is an interesting result that shows that the long-time component of polar solvation dynamics is equal to the residence time of the water molecules.

9.7 Rotational friction on an aqueous globular protein: role of hydration shell dynamics

The hydrodynamic radius (obtained from the Stokes–Einstein–Debye relations) of an aqueous globular protein is often found to be substantially greater than its actual radius. This increase in radius is explained pictorially in terms of a hydration shell around the protein. However, there is as yet no satisfactory quantitative explanation of the enhanced friction on the protein's motion in terms of the *dynamic characteristics* of the water in the shell.

The Debye–Stokes–Einstein (DSE) relation between the rotational diffusion coefficient (D_R) and the radius (R) is given by:

$$D_R = k_B T / 8\pi\eta R^3 \tag{18}$$

Here η is the viscosity of bulk water and $k_B T$ is the product of the Boltzmann constant and the temperature T. The DSE ralation is found to be inadequate—it predicts too small values for R if the experimental values of D_R are used in eqn. (18). A size much larger than R needs to be used in the above equation to obtain agreement with experimental results. For example, for myoglobin, if one uses the radius of 16.5 Å (computed from its volume), one finds an orientational correlation time (equal to $(2D_R)^{-1}$) of 14 ns while the observed value is 45 ns. Therefore, DSE relation would require a value of radius that is about 50% larger than the actual value. A similar large enhancement is required for most of the globular proteins. By using Kirkwood's well-known expression for friction,[70] one can derive a simple expression for the friction due to the hydration layer:[223]

$$\xi_{P,bw} = (8\pi\beta/9) R^2 L_H \rho Q_{eff}^2 \mu^2 <\tau_T> / (\varepsilon_L^2 <r>^4). \tag{19}$$

For myoglobin, the radius is 16.5 Å.[22,23] If one uses L_H = 6 Å, μ = 1.8 D, $\rho = 3.3 \times 10^{22}$ cm^{-3}, $<r>$ = 4 Å, ε_L = 5, T = 300 K, η = 0.01 Poise, τ_T = 50 ps, Q_{eff} = 1 esu and R = 16.5 Å, a value of the biological water contribution ($\xi_{P,bw}$) equal to $1.9\xi_{P,hyd}$ is obtained. That is, the total friction is equal to $2.9\xi_{P,hyd}$. This in turn gives a value of the rotational correlation function equal to 41 ns which is very close to the experimental value of 45 ns for myoglobin.

10 Water solvation dynamics in self-organized assemblies

The success in the investigation of solvation dynamics in bulk water motivated many such studies on complex systems where water is an important ingredient. In addition to studies of proteins and DNA, a large number of experimental studies and several computer simulations have been directed towards understanding water dynamics in self-organized assemblies through studies of solvation dynamics of suitably placed probes. The organized assemblies include self-assembled molecular aggregates in polar liquids (*e.g.* micelles[44–48] or vesicles[55,56] in water) or nonpolar liquids (*e.g.* reverse micelles[49–52] or microemulsions[52–54] in hydrocarbons), cage-like hosts soluble in many liquids (cyclodextrins[70,224] or calixarenes) and semi-rigid materials (*e.g.* polymers[57–61]). The modern era of solvation dynamics in organized assemblies began with the well-known work of Vajda *et al.*[70] who found that the solvation dynamics of the Coumarin probe within a cyclodextrin cavity slow down substantially in the long term. This slow down is attributed to the quenching of the translational motion of the water molecules inside the cavity. A conclusive understanding may require a detailed computer simulation, but it is clear that the dynamics in a restricted environment can slow down dramatically compared to that in the bulk. In the following, we shall discuss the dynamics of water in micelles, reverse micelles, polymer hydrogels and a few other systems.

10.1 Computer simulations of water dynamics in self-organized assemblies

There have been several interesting computer simulation studies aimed at understanding water dynamics in organized assemblies. In an early simulation, Stillinger and coworkers[225] reported that the dynamics of a water molecule at the surface of a hydrophobic solute is about 20% slower than that in the bulk. In an interesting simulation, Senapati and Chandra[226] simulated water inside a cavity and showed that the dielectric constant of confined water can be significantly smaller than that of the bulk, extended water. They also found a marked slowing down in the solvation dynamics of confined water. Ladanyi and coworkers[227,228] reported a detailed simulation of solvation dynamics inside the water pool of an aqueous reverse micelle, which was held rigid. The solvation dynamics shows no noticeable slowing down. This may be due to the fact that the simulation run was limited to only 10 ps. Berne *et al.*[85] showed that one of the reasons of the high dielectric constant of liquid water is the large contribution to dipole moment fluctuation arising from the large polarizability of the individual water molecules (the dipole induced effect). In an organized assembly, this polarization effect can get reduced because a large fraction of water molecules are surrounded by less polarizable groups. This may result in a large decrease in the value of the dielectric constant. Note that this effect is in addition to the decrease observed by Senapati *et al.*[226] where the decrease in dielectric constant is due to the suppression of the long-wavelength moment fluctuation.

Several simulations have been carried out to explore water dynamics on the surface of a micelle. Klein and coworkers[229,230] and Pal *et al.*[231] reported a slowing down in the water orientational relaxation in the surface of a micelle. Balasubramanian *et al.* carried out fully atomistic MD simulations of a micelle consisting of caesium perfluorooctanoate (CsPFO) surfactant molecules in water.[232] The CsPFO micelle is stable over a wide temperature range for the duration of the simulation (5 ns). They studied orientational relaxation, hydrogen bond lifetime and also solvation dynamics of the natural probe Cs^+ ions at the interface. Dramatic slowing down of water dynamics was observed in all cases. In Fig. 23, the orientational correlation function of the interfacial water is shown and compared with the same for bulk water. The average is carried out over the water molecules which are within 4.5 Å from the nearest surface atom. Note the dramatic slow decay in the long time. In the top-half of the same figure, the time dependence of the dipolar correlation function at short times is shown at several distances. The decay becomes faster as the water molecules are located at larger distances from the interface.

In Fig. 24, the solvation time correlation function of a Cs^+ ion at the interface is shown. For comparison, the same correlation function now computed in the bulk is shown in the inset. Note the large difference in the time scale of the decay. An analysis of the dynamics of water at the interface reveals the following facts. (a) The hydrogen bond lifetime of the bonds between water and the polar head groups (PHG) at the surface is longer (by about a factor 5–10) than that between any two water molecules. The hydrogen bond lifetime correlation functions $C_L(t)$ and $S_L(t)$ are shown in Fig. 25. This figure can be compared with Fig. 3 where the same functions are shown for bulk water. This result indicates the presence of quasi-bound water molecules on the surface. The lifetime of the latter is also increased by about 25% near the surface.[84] (b) Dynamics of water molecules at the interface is in general slower than those in the

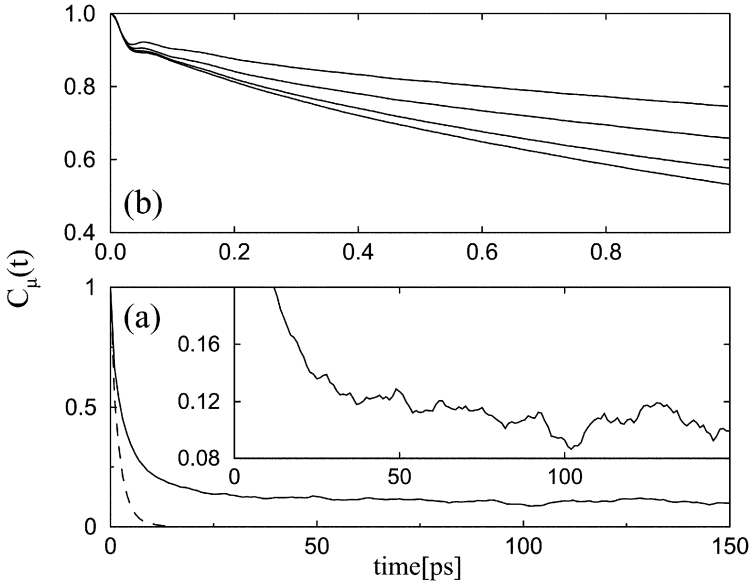

Fig. 23 The dipolar orientational correlation function of interfacial water. The average is carried out over all the water molecules which are within 10 Å from the nearest surface atom. Note the slow decay in the long term. The dashed line shows the decay for water molecules in the bulk. (Top) The time dependence of the dipolar correlation function at short times is shown at four distances from the surface. These are (from the top): 4.5, 6, 10 and 28 Å). The decay becomes faster as the water molecules are located at increasingly larger distances from the micellar surface.

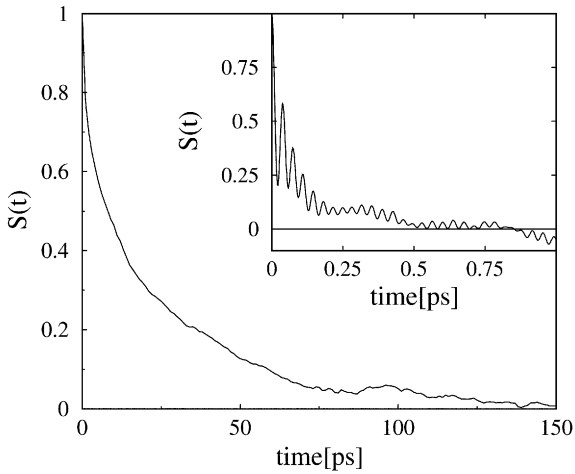

Fig. 24 Computed solvation time correlation function of interfacial Cs^+ ions. The average has been carried out over all the water Cs^+ ions which are within 10 Å from the nearest surface atom. For comparison, we show in the inset the solvation dynamics of Cs^+ ions in bulk water.

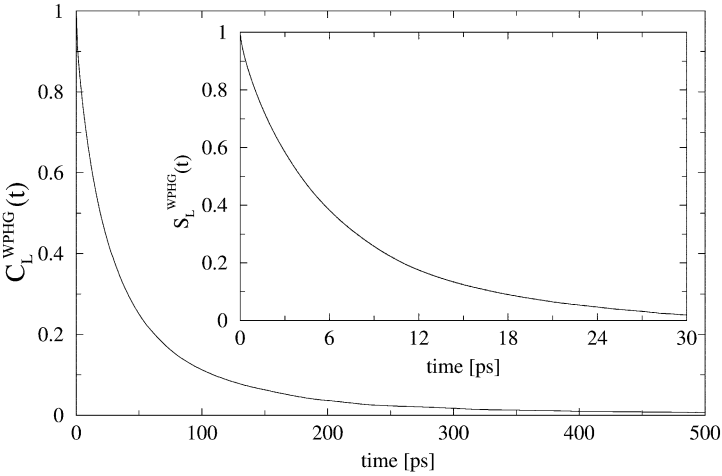

Fig. 25 The hydrogen bond lifetime correlation functions ($C_L(t)$ and $S_L(t)$) for the hydrogen bond between the polar head group (PHG) of the CsPFO micelle and a water molecule at the interface. This figure should be compared with Fig. 3 where the same lifetime correlation functions are shown for two water molecules in the bulk.

bulk and the approach to bulk behaviour as one moves away from the micellar surface is slow. (c) The hydrogen bond between PHG and water molecules is much stronger than that between any two water molecules. (d) Water molecules at the surface can be categorized as free (IFW—interfacial free water), singly hydrogen bonded to a PHG (IFB1—interfacial singly hydrogen bonded) and doubly hydrogen bonded (IFB2) species, each with well-defined lifetimes and the population ratio is 1 : 8 : 1, that is singly bonded species are dominant.[232] This is a bit surprising because the doubly H-bonded species are energetically most favoured. The reason for this is attributed to entropy.

In a very recent simulation study Pal *et al.* showed that the frequency of the libration mode of the hydrogen atoms and the frequency of the O–O–O bending mode undergo a substantial blue shift for bound water molecules at the anionic micellar surface.[233] However, the frequency of the O–O stretch remains unchanged at 200 cm^{-1}. These results are in very good agreement with the inelastic incoherent neutron scattering (IINS) data on aqueous protein solutions where a similar blue shift has been observed for the two modes mentioned above. This blue shift is attributed to the enhanced rigidity of water at the micellar interface.

Recently, Berkowitz and coworkers[234,235] have also employed molecular dynamics simulations to study the structure and dynamics of a sodium dodecyl sulfate micelle in water. Their detailed simulations add to the knowledge of this system obtained from earlier simulations of Klein and coworkers,[236] and that of Mackerell.[237] Here also the water molecules at the interface form hydrogen bonds with the head groups of the surfactant, apart from forming hydrogen bonds with other water molecules. About 60% of the interfacial water molecules are singly hydrogen bonded with the micelle, while 33% form two such hydrogen bonds. A small fraction of the molecules do not form any hydrogen bonds with the micelle. The reorientational time correlation

function for the dipoles of the water molecules within a 6 Å hydration layer exhibits slow relaxation, and a long lived plateau that results from the loss of orientational freedom for such water molecules, in agreement with the results obtained by Balasubrmanian *et al.*[232]

10.2 Dielectric relaxation of micelles, reverse micelles and microemulsions

Several relaxation times in the long (μs), intermediate (10 ns) and fast (0.1–0.3 ns) time scales have been detected by Telgmann and Kaatze in micelles using ultrasonic absorption in the 100 kHz to 2 GHz frequency range.[238] The longest relaxation time is attributed to the exchange of monomers between the bulk and the micelles while the fastest to the rotation of the alkyl chains of the surfactants in the core of the micelle. The intermediate relaxation time has not been assigned to any particular motion. Recent dielectric relaxation studies of bound water in reverse micelles provide information on the mobility of the water molecules in the nanometer-sized pools.[239,240] THz spectroscopic studies in the frequency range 0.2–2 THz show that the amplitude of the dielectric relaxation in the water pool is substantially smaller than that in bulk water.[239] *It is suggested that confinement, rather than local structure of the hydrogen-bonded network, is responsible for the suppression of the relaxation amplitude and that within the water pool, the "free" water is not structurally equivalent to the bulk water.* [239] Dielectric relaxation of an AOT–water–carbon tetrachloride (CCl_4) microemulsion in the 0.02–3 GHz frequency range as a function of the water to AOT molar ratio ($0.2 < w_0 < 10$) has been reported.[240] A single relaxation time (about 7 ns at the lowest water content, $w_0 = 0.2$) was observed which becomes greater with an increase in w_0.

10.3 Solvation dynamics in organized assemblies

Understanding of solvation dynamics in these systems faces several difficulties. First, the location of the probe can be unclear, one could thus measure an average over several possible locations of the probe. Second, due to molecular diffusion, a probe molecule undergoes an excursion over a region with a radius of a few nm within its excited state lifetime of several nanoseconds. Thus a fluorescent probe actually reports the property of a microenvironment, with a radius of a few nm.[241–243]

10.3.1 Solvation dynamics in micelles. Micelles have a dense hydrophobic core while the polar head groups (PHG) are on the surface. It is expected that water molecules on the surface are constrained by hydrogen bonding with the PHGs. However, the extent of this effect is not clear. An additional complexity in this case is that there are three possible locations of the probe, namely the bulk water, the "dry" micellar core and the Stern layer. Solvation dynamics in micelles have been studied using Coumarin 480 (C480) and 4-aminophthalimide (4-AP) as probes.[244,245] Emission properties of the probes in the micelles are very different from those in water and in hydrocarbons,[244,245] indicating that the probes reside neither in bulk water nor in the core of the micelles and hence, are located in the Stern layer of the micelles. Sarkar *et al.*[244] and Datta *et al.*[245] studied solvation dynamics of C480 and 4-AP, respectively, in

neutral (TX-100), cationic (CTAB) and anionic (SDS) micelles. It is observed that for SDS, CTAB and TX-100 the average solvation times are respectively 180, 470 and 1450 ps for C480[244] and 80, 270 and 720 ps for 4-AP.[245] Thus, the solvation dynamics in the Stern layer of micelles is two orders of magnitude slower than that in the bulk water, about 10 times faster than that in the water pool of the microemulsions[244,245] and is slightly faster than the longest component of the solvation dynamics in γ-CD. For both the probes, it is observed that the solvation times occur in the order TX > CTAB > SDS. Qualitatively, the difference in the solvation times in the three micelles may be ascribed to the differences in their structures[246–249]—the thickness of the hydrated shell for TX-100 (25 Å) is higher than that for SDS and CTAB (6–9 Å). The SANS studies indicate CTAB micelles are drier than SDS micelles.[246–249] It is interesting to note that the time scale of solvation is similar to the intermediate range of dielectric relaxation times reported by Telgmann and Kaatze.[238]

10.3.2 Solvation dynamics in reverse micelles and microemulsions. Reverse micelles and microemulsions have a water pool in the core and hydrocarbon chains outside. The emission spectrum of the probe changes markedly when it is transferred from the bulk hydrocarbon to the water pool. The absorption maxima of Coumarin 480 (C480) in *n*-heptane and water are at 360 and 395 nm, respectively, while the emission maxima are at 410 and 490 nm, respectively.[250] Addition of AOT and subsequently water to an *n*-heptane solution of C-480 results in a very prominent shoulder at 480 nm.[251] which can, therefore, be easily assigned to the C480 molecules in the water pool of the microemulsion. Sarkar *et al.* studied the solvation dynamics of C480 in AOT/*n*-heptane/water microemulsions.[251] They observed a distinct rise time in the nanosecond time scale at the red end of the emission spectra. They observed that in a small water pool ($w_0 = 4$, $r_w = 8$ Å) the solvation time is 8 ns while for a very large water pool ($w_0 = 32$, $r_w = 64$ Å) the response is bimodal with a fast component of 1.7 ns and a slower component of 12 ns. As shown in Fig. 26, these studies missed all of the ultrafast solvation which occurs on the ps (or faster) time scale. Bright and coworkers studied the solvation dynamics of acrylodan-labeled human serum albumin in an AOT microemulsion by phase fluorimetry.[252] They reported that the solvation time is about 8 ns for a small water pool ($w_0 = 2$) and 2 ns for a large water pool ($w_0 = 8$). In order to explore the effects of ions, Mandal *et al.*[253] studied the solvation dynamics of 4-AP in a microemulsion containing the neutral surfactant triton X-100 where no ions are present in the water pool. The triton X-100 microemulsion also exhibits nanosecond solvation dynamics.

Levinger *et al.* studied the solvation dynamics of a charged dye Coumarin 343 (C343) in lecithin and AOT microemulsions using femtosecond upconversion.[254–257] For lecthin microemulsions,[254] the solvent relaxation displays a very long component which does not become complete within 477 ps. This observation is similar to the nanosecond dynamics reported by Bright *et al.*[252] and Sarkar *et al.*[251] For Na-AOT, the solvation dynamics reported by Levinger *et al.*[256] for the charged probe C343 are faster than those reported by Bright and coworkers[252] and Sarkar *et al.*.[251] Shirota and Horie[258] have also demonstrated that in the AOT microemulsions the solvation dynamics of acetonitrile and methanol are non-exponential and 1000 times slower

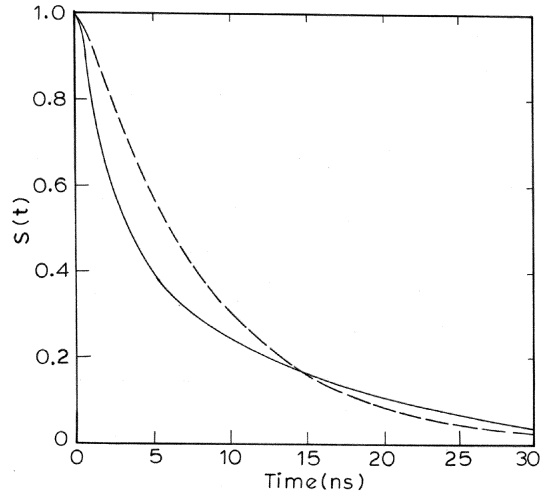

Fig. 26 Solvation time correlation function for the solvation of Coumarin 480 dye in the water pool of reverse micelle AOT/*n*-heptane at water contents $w_0 = 4$ (dashed line) and $w_0 = 32$ (solid line), as obtained from the experiment of Sarkar *et al.*.

when compared to those in the pure solvents. They attributed the non-exponential decay to the inherent inhomogeneous nature of the solvent pools.

10.3.3 Solvation dynamics in lipid vesicles. A lipid vesicle resembles a biological cell. It contains an aqueous volume enclosed within a membrane and dispersed in bulk water. Red edge excitation spectroscopy (REES)[131,132] has been used to study the state of solvation of a fluorescent probe, in the ground state, in uni-lamellar and multi-lamellar vesicles. Datta *et al.* observed that the solvation dynamics of C480 in dimiristoylphosphaticholine (DMPC) vesicles are highly non-exponential with two components of 0.6 ns (40%) and 11 ns (60%).[259] This result is very similar to the solvation dynamics of the same probe in the large water pools of AOT micro-emulsions.[251,252] The nanosecond solvation dynamics in lipids cannot be due to the chain dynamics of DMPC which occur on the 100 ns time scale.[260–262]

11 Concluding remarks and future problems

The present Report attempts to survey the current status of the theoretical, experimental and computer simulation studies on solvation dynamics of water both in its neat state as well as in complex chemical and biological systems. The recently discovered ultrafast, sub-50 fs solvation component in bulk water has been reviewed in detail. We have addressed the role of the intermolecular vibrational modes of water in this ultrafast solvation. The existence of ultrafast solvation in water has significant consequencesd in several other dynamic processes in water. We have discussed how the ultrafast solvation reduces the magnitude of dielectric friction on the motion of small

rigid ions like Li^+, Na^+ *etc*. The theoretical value is now in good agreement with the long known experimental values of limiting ionic conductivity. We have also discussed the effects of this ultrafast solvation on the electron transfer reaction. Here, this ultrafast component seems to provide a good explanation for the observed lack of dynamic solvent effects on many adiabatic electron transfer reactions in water. Recent theoretical studies have also provided an elegant explanation of the seemingly anomalous concentration dependence of the solvation rate in aqueous electrolyte solutions that has been observed in recent years.

In the second part of the Report, attention has been focused on complex systems that include biomolecules, like proteins, as well as self-organized molecular assemblies such as micelles, reverse micelles, vesicles, *etc*. The experimental, theoretical and simulation studies clearly demonstrate that the dynamics of water present either in the vicinity of, or entrapped within, the structure of these complex systems are significantly different from those of bulk water. The most remarkable effect is the dramatic slow down in the long time decay of the *orientational* correlation function of the water molecules at the surface of a protein or a self-assembly. This slow down persists even in the average over all of the surface molecules. This slow down is also observed in the solvation dynamics of the probe as well. However, one fails to notice such a significant signature in the translational diffusion which slows down only by 25% or so. The explanation for this disparity is simple—translational diffusion is a much slower process. The transient hydrogen bonding and concomitant transient localization does not affect the slow process of translational diffusion.

The above advancement in the study of water solvation dynamics in complex systems has given rise to several extremely interesting problems for future studies. A list with a brief discussion of each suggested problem is given below.

11.1 Protein-glass transition at 200 K: Role of water dynamics

Neutron scattering and computer simulation studies have shown that all proteins undergo a glass transition at around 200 K.[263–265] Experiments and simulations show that below this temperature, the dynamic behaviour of proteins change from anharmonic to harmonic. It has been anticipated that below this temperature, proteins form a glassy state. It should be noted that most proteins, the enzymatic activity ceases below 220 K.[266,267] It has been argued that water dynamics may hold the key to the understanding of this unusual behaviour of proteins. Note that water itself is believed to have a glass transition of around 135 K.[268] It has also been suggested that water also has a transition temperature of 228 K below it behaves like a strong liquid while above this temperature, it behaves like a fragile liquid.[269] The proximity of this liquid–liquid transition to the protein glass transition temperature is highly suggestive. Clearly, at temperatures below 220 K or so, the dynamics of water and protein are highly coupled. A recent computer simulation has shown that the structural relaxation of a protein requires relaxation of the water hydrogen bond network and the translational displacement of surface water molecules.[270] It is, therefore, clear that the dynamics of water at the interface can play a very important role. This is an interesting problem that deserves further study.

11.2 Water mediated molecular recognition

The recognition of binding sites (the 'sticky' regions) of proteins by ligands, inhibitors, substrates and other proteins is expected to control, to some extent, the biological activity of proteins.[271] It is clear that the hydrophilic sites of a protein will be covered by slow water molecules while the dynamics of water molecules near the hydrophobic residues are not expected to be substantially perturbed. As a ligand approaches a protein, an important step towards binding may occur in a short time (in a few tenths of a picosecond) when the surface water molecules will determine the rate, and even the outcome of binding.

A microscopic theory of molecular recognition would need to discuss the free energy barrier (or rather, free energy landscape) at the surface that will be experienced by the incoming ligand. Experiments by Zewail and coworkers[272] have already given an indication of the need of such a molecular level description. In their study of molecular recognition by a protein mimic, the cobalt picket-fence porphyrin, Zewail *et al*.[272] found the need to assume an energy landscape which involves two barriers. The first step is the "absorption" of O_2 in the hydration layer of the protein which is followed by the subsequent binding. This may be a common mechanism in many other cases. A more microscopic treatment of such phenomena will require the inclusion of hydration dynamics at the interface.

11.3 Protein folding and protein association: Role of biological water

The dynamics of water around an extended, unfolded protein certainly play a very important role in determining the rate of protein folding. For example, hydrophobic collapse involves movement of water molecules away from the region between two hydrophobic amino acid residues that form a pair contact. Similarly, beta bends also involve water mediation. In both of these examples, the water molecules in close proximity to the protein amino acids are expected to play a critical role. This role will involve a subtle balance between enthalpic and entropic forces. For example, it is found that doubly bonded water molecules in the micellar surface are relatively rare, although energetically favourable.

Water molecules in the protein hydration layer have a finite residence time. This residence time has a distribution, depending on the nature of the neighbouring protein surface, and this distribution can play a critical role in protein association. The final act of association of two proteins may require partial desolvation around the necessary amino acid residue sites.[273] This is only possible if the residence time of water around these sites is sufficiently short. The residence time is determined by the dynamics in the hydration layer. This correlation between hydration layer and protein association is also an important problem that deserves further study.

11.4 Origin of the ultraslow component

The observation of the very slow (~(1–10) ns)) component in the solvation dynamics of an external probe in micelles, reverse micelles and other self-organized assemblies

has still defied a satisfactory explanation.[12,13] Note that such a slow component is absent in protein hydration dynamics when a natural probe located near the surface is used. In such cases, the slowest time observed is just about 40 ps. The ultra-slow component has also not been observed in the computer simulation studies of solvation dynamics in micelles and reverse micelles. In the latter cases, the slowest component is again less than 100 ps. One can think of at least two mechanisms that could give rise to decay on the ns time scale. First, the solute probe may itself diffuse after photo-excitation. The free energy for probe re-distribution comes from the creation of the large dipole moment in the probe. Second, the bound $\leftrightarrow$ free water equilibrium may still be relevant but now the bound water may be trapped inside the hydrocarbon core. This is possible in TX-100 a neutral micelle which has a thick hydration shell. Such water molecules will be slow to orient in response to the external field as they would need to overcome packing and would need to break hydrogen bonds. This is certainly a worthwhile problem to pursue—both experimentally and theoretically.

The above list is by no means exhaustive, but it is hoped that it gives a glimpse of many interesting (and challenging, although often very difficult) problems that remain to be understood in the area of water solvation dynamics in complex aqueous systems. This field will surely be an active area of research in the future and one can look forward to many exciting new results.

Acknowledgements

It is a pleasure to thank Mr Dwaipayan Chakrabarti, Mr. Prasanth Jose and Mr. Arnab Mukherjee for much help in preparing this manuscript. I thank Professors S. Balasubramanian, Ranjit Biswas, Amalendu Chandra, Graham Fleming, Nilashis Nandi, Srabani Roy and Mr. Subrata Pal for collaboration in the general area of solvation dynamics. It is a pleasure to thank Professors Paul Barbara, Kankan Bhattacharyya, Graham Fleming, Mark Maroncelli, Iwao Ohmine, Ahmed Zewail and Bob Zwanzig for many discussions over the years. This work was supported in parts by grants from the Department of Science and Technology (DST), India, and the Council of Scientific Research (CSIR), India.

References

1 G. R. Fleming and P. G. Wolynes, *Physics Today*, (Special Issue) May 1990, p. 36.
2 (*a*) P. F. Barbara and W. Jarzeba, *Adv. Photochem*, 1990, **15**, 1; (*b*) P. F. Barbara and W. Jarzeba, *Acc. Chem. Res.*, 1988, **21**, 195.
3 M. Maroncelli, J. McInnis and G. R. Fleming, *Science*, 1989, **243**, 1674.
4 B. Bagchi, *Annu. Rev. Phys. Chem.*, 1989, **40**, 115.
5 P. J. Rossky and J. D. Simon, *Nature (London)*, 1994, **370**, 263.
6 G. R. Fleming and M. Cho, *Annu. Rev. Phys. Chem.*, 1996, **47**, 109.
7 G. R. Fleming, T. Joo and M. Cho, *Adv. Chem. Phys.*, 1997, **101**, 141.
8 P. J. Rossky and J. Schnitker, *J. Phys. Chem.*, 1988, **92**, 4277.
9 S. K. Pal, J. Peon, B. Bagchi and A. H. Zewail, *J. Phys. Chem. B*, 2002, **106**, 12376.
10 B. Bagchi and A. Chandra, *Adv. Chem. Phys.*, 1991, **80**, 1.
11 N. Nandi, K. Bhattacharyya and B. Bagchi, *Chem. Rev.*, 2000, **100**, 2013.
12 K. Bhattacharyya and B. Bagchi, *J. Phys. Chem. A*, 2000, **104**, 10603.

13 (*a*) B. Bagchi and R. Biswas, *Adv. Chem. Phys.*, 1999, **109**, 207; (*b*) B. Bagchi and R. Biswas, *Acc. Chem. Res.*, 1998, **31**, 181.
14 I. Benjamin, *Chem. Rev.*, 1996, **96**, 1449.
15 H. Heitele, *Angew. Chem., Int. Ed. Engl.*, 1993, **32**, 359.
16 B. Bagchi, D. W. Oxtoby and G. R. Fleming, *Chem. Phys.*, 1984, **86**, 257.
17 G. van der Zwan and J. T. Hynes, *J. Phys. Chem.*, 1985, **89**, 4181.
18 M. Maroncelli, *J. Mol. Liq.*, 1993, **57**, 1.
19 H. L. Friedman, F. O. Raineri and H. Resat, in *Molecular Liquids*, ed. J. Teixeira-Diaz, NATO-ASI Ser., Kluwer Academic Publishers, Amsterdam, 1992, p. 183.
20 R. M. Stratt and M. Maroncelli, *J. Phys. Chem.*, 1996, **100**, 12981.
21 N. Nandi and B. Bagchi, *J. Phys. Chem. B*, 1997, **101**, 10954.
22 *Protein–Solvent Interactions*, ed. R. B. Gregory, Marcel Dekker, Inc., New York, 1995.
23 R. Pethig, *Annu. Rev. Phys. Chem.*, 1992, **43**, 177.
24 See ch. 7 in *Water in Biology, Chemistry and Physics*, ed. G. W. Robinson, S. B. Zhu, S. Singh and M. W. Evans, World Scientific, Singapore, 1996.
25 See papers in *J. Mol. Liq.* (Special Issue: Water at the New Millennium), ed. M. Besnard and R. Buchner, Elsevier, Amsterdam, 2002, vol. 101.
26 V. Makarov, B. M. Pettitt and M. Feig, *Acc. Chem. Res.*, 2002, **35**, 376.
27 Y.-K. Cheng and P. J. Rossky, *Nature(London)*, 1998, **392**, 696.
28 M. M. Teeter, *Annu. Rev. Biophys. Chem.*, 1991, **20**, 577.
29 V. A. Makarov, M. Feig, B. K. Andrews and B. M. Pettitt, *Biophys. J.*, 1998, **75**, 150.
30 G. Otting, E. Liepinsh and K. Wüthrich, *Science*, 1991, **254**, 974.
31 (*a*) B. Halle, T. Anderson, S. Forsén and B. Lindman, *J. Am. Chem. Soc*, 1981, **103**, 500; (*b*) B. Halle, *Mol. Phys.*, 1984, **53**, 1427; (*c*) B. Halle, *Mol. Phys.*, 1985, **56**, 209.
32 (*a*) L. A. Halliday and M. R. Topp, *Chem. Phys. Lett.*, 1978, **48**, 40; (*b*) L. A. Halliday and M. R. Topp, *J. Phys. Chem.*, 1977, **82**, 2273.
33 H. E. Lessing and M. Reichert, *Chem. Phys. Lett.*, 1977, **46**, 111.
34 T. Okamura, M. Sumitani and K. Yoshihara, *Chem. Phys. Lett.*, 1983, **94**, 339.
35 E. W. Castner, B. Bagchi, M. Marocelli, S. P. Webb, A. J. Ruggiero and G. R. Fleming, *Ber. Bunsenges. Phys. Chem.*, 1988, **92**, 363.
36 V. Nagarajan, A. M. Brearley, T.-J. Kang and P. F. Barbara, *J. Chem. Phys.*, 1987, **86**, 3183.
37 M. Maroncelli and G. R. Fleming, *J. Chem. Phys.*, 1987, **86**, 6221.
38 M. A. Kahlow, T.-J. Kang and P. F. Barbara, *J. Chem. Phys.*, 1988, **88**, 2372.
39 M. A. Kahlow, W. Jarzeba, T.-J. Kang and P. F. Barbara, *J. Chem. Phys.*, 1989, **90**, 151.
40 E. Castner, M. Maroncelli and G. R. Fleming, *J. Chem. Phys.*, 1987, **86**, 1090.
41 S.-G. Su and J. D. Simon, *J. Chem. Phys.*, 1987, **91**, 2693.
42 R. Jimenez, G. R. Fleming, P. V. Kumar and M. Maroncelli, *Nature (London)*, 1994, **369**, 471.
43 M. J. Lang, X. J. Jordanides, X. Song and G. R. Fleming, *J. Chem. Phys.*, 1999, **110**, 5584.
44 S. K. Pal, D. Sukul, D. Mandal, S. Sen and K. Bhattacharyya, *Chem. Phys. Lett.*, 2000, **327**, 91.
45 D. Mandal, S. Sen, T. Tahara and K. Bhattacharyya, *Chem. Phys. Lett.*, 2002, **359**, 77.
46 K. Hara, H. Kuwabara and O. Kajimoto, *J. Phys. Chem. A*, 2001, **105**, 7174.
47 C. Ju and C. Bohne, *J. Phys. Chem.*, 1996, **100**, 3847.
48 S. Sen, P. Dutta, S. Mukherjee and K. Bhattacharyya, *J. Phys. Chem. B*, 2002, **106**, 7745.
49 D. S. Venables, K. Huang and C. A. Schmuttenmaer, *J. Phys. Chem. B*, 2001, **105**, 9132.
50 J.-B. Brubach, A. Mermut, A. Filabozzi, A. Gerschel, D. Lairez, M. P. Kraft and P. Roy, *J. Phys. Chem. B*, 2001, **105**, 430.
51 N. E. Levinger, *Curr. Opin. Colloid Interface Sci.*, 2000, **5**, 118.
52 S. K. Pal, D. Mandal, D. Sukul and K. Bhattacharyya, *Chem. Phys. Lett.*, 1999, **312**, 178.
53 K. Bhattacharyya, K. Hara, N. Kometani, Y. Yozu and O. Kajimoto, *Chem. Phys. Lett.*, 2002, **361**, 136.
54 S. Sen, D. Sukul, P. Dutta and K. Bhattacharyya, *J. Phys. Chem. A*, 2002, **106**, 6017.
55 J. Sykora, P. Kapusta, V. Fidler and M. Hof, *Langmuir*, 2002, **18**, 571.
56 S. K. Pal, D. Sukul, D. Mandal and K. Bhattacharyya, *J. Phys. Chem. B*, 2000, **104**, 4529.
57 R. Narenberg, J. Kliger and D. Horn, *Angew Chem., Int. Ed.*, 1999, **38**, 1626.
58 S. Sen, D. Sukul, P. Dutta and K. Bhattacharyya, *J. Phys. Chem. B*, 2002, **106**, 3763.
59 P. Dutta, S. Sen, S. Mukherjee and K. Bhattacharyya, *Chem. Phys. Lett.*, 2002, **359**, 15.
60 L. Frauchiger, H. Shirota, K. E. Uhrich and E. W. Castner Jr., *J. Phys. Chem. B*, 2002, **106**, 7463.
61 H. Shirota and E. W. Castner Jr., *J. Am. Chem. Soc.*, 2001, **123**, 12877.
62 X. J. Jordandies, M. J. Lang, X. Song and G. R. Fleming, *J. Phys. Chem. B*, 1999, **103**, 7995.
63 S. K. Pal, D. Mandal, D. Sukul, S. Sen and K. Bhattacharyya, *J. Phys. Chem. B*, 2001, **105**, 1438.
64 D. Zhong, S. K. Pal and A. H. Zewail, *Chemphyschem*, 2001, **2**, 219.
65 (*a*) S. K. Pal, J. Peon and A. H. Zewail, *Proc. Natl. Acad. Sci. USA.*, 2002, **99**, 1763; (*b*) J. Peon, S. K. Pal and A. H. Zewail, *Proc. Natl. Acad. Sci. USA*, 2002, **99**, 10964.
66 D. Mandal, S. Sen, D. Sukul, K. Bhattacharyya, A. K. Mandal, R. Bannerjee and S. Roy, *J. Phys. Chem.*, 2002, **106**, 10741.
67 B. B. Brauns, C. J. Murphy and M. Berg, *J. Am. Chem. Soc.*, 1998, **120**, 2449.

68 B. B. Brauns, M. L. Madaras, R. S. Coleman, C. J. Murphy and M. A. Berg, *J. Am. Chem. Soc.*, 1999, **121**, 11644.
69 B. B. Brauns, M. L. Madaras, R. S. Coleman, C. J. Murphy and M. A. Berg, *Phys. Rev. Lett.*, 2002, **88**, 158101.
70 S. Vajda, R. Jimnez, S. J. Rosenthal, V. Fidler, G. R. Fleming and E. W. Castner, Jr., *J. Chem. Soc., Faraday Trans.*, 1995, **91**, 867.
71 N. Nandi and B. Bagchi, *J. Phys. Chem.*, 1996, **100**, 13914.
72 I. Ohmine and H. Tanaka, *Chem. Rev.*, 1993, **93**, 2545.
73 I. Ohmine, *J. Phys. Chem.*, 1995, **99**, 6767.
74 M. Cho, G. R. Fleming, S. Saito, I. Ohmine and R. M. Stratt, *J. Chem. Phys.*, 1994, **100**, 6672.
75 L. Thrane, R. H. Jacobsen, P. Uhd Jepsen and S. R. Keiding, *Chem. Phys. Lett.*, 1995, **240**, 330.
76 S. Palese, S. Mukamel, R. J. D. Miller and W. T. Lotshaw, *J. Phys. Chem.*, 1996, **100**, 10380.
77 D. McMorrow and W. T. Lotshaw, *Chem. Phys. Lett.*, 1990, **174**, 85.
78 J. Barthel, K. Bachhuber, R. Buchner and H. Hetzenauer, *Chem. Phys. Lett.*, 1990, **165**, 369.
79 S. Palse, L. Schilling, R. J. D. Miller, R. Staver and W. T. Lotshaw, *J. Phys. Chem.*, 1994, **99**, 6308.
80 F. H. Stillinger, *Adv. Chem. Phys.*, 1975, **31**, 1.
81 A. Luza and D. Chandler, *Phys. Rev. Lett.*, 1996, **76**, 928.
82 A. Luzar, *J. Chem. Phys.*, 2000, **113**, 10663.
83 A. Chandra, *Phys. Rev. Lett.*, 2000, **85**, 768.
84 S. Balasubramanian, S. Pal and B. Bagchi, *Phys. Rev. Lett.*, 2002, **89**, 115505.
85 S. W. Rick, S. J. Stuart and B. J. Berne, *J. Chem. Phys.*, 1994, **101**, 6141.
86 J. Barthel and R. Buchner, *Pure. Appl. Chem.*, 1991, **63**, 1473.
87 J. T. Kindt and C. A. Schmuttenmaer, *J. Phys. Chem.*, 1996, **100**, 10373.
88 J. B. Hasted, S. K. Husain, F. A. M. Frescura and R. Birch, *Chem. Phys. Lett.*, 1985, **118**, 622.
89 D. Bertolini and A. Tani, *Mol. Phys.*, 1992, **75**, 1047.
90 B. Guillot, *J. Chem. Phys.*, 1991, **95**, 1543.
91 (*a*) M. Neuman, *J. Chem. Phys.*, 1985, **82**, 5663; (*b*) M. Neuman, *J. Chem. Phys.*, 1988, **85**, 1567.
92 E. L. Pollack and B. J. Alder, *Annu. Rev. Phys. Chem.*, 1981, **32**, 311.
93 G. Williams, *Chem. Rev.*, 1972, **72**, 55.
94 B. Guillot, *J. Mol. Liq.*, 2002, **101**, 217.
95 J. B. Hasted, S. K. Husain, F. A. M. Frescura and J. R. Birch, *Infrared Phys.*, 1987, **27**, 11.
96 M. N. Afsar and J. B. Hasted, *Infrared Phys.*, 1978, **18**, 835.
97 G. M. Hale and M. R. Querry, *Appl. Opt.*, 1973, **12**, 555.
98 J. E. Bertie, K. M. Ahmed and H. H. Eysel, *J. Phys. Chem.*, 1989, **93**, 2210.
99 N. Nandi, S. Roy and B. Bagchi, *J. Chem. Phys.*, 1995, **102**, 1390.
100 M. S. Skaf and B. M. Ladanyi, *J. Chem. Phys.*, 1995, **102**, 6542.
101 B. M. Ladanyi and M. S. Skaf, *J. Phys. Chem.*, 1996, **100**, 1368.
102 F. O. Raineri and H. L. Friedman, *J. Chem. Phys.*, 1993, **98**, 8910.
103 F. O. Raineri, H. Resat, B. C. Perng, F. Hirata and H. L. Friedman, *J. Chem. Phys.*, 1994, **100**, 1477.
104 Y. Zhou, H. L. Friedman and G. Stell, *J. Chem. Phys.*, 1989, **91**, 4885.
105 F. O. Raineri, Y. Zhou, H. L. Friedman and G. Stell, *Chem. Phys.*, 1991, **152**, 201.
106 F. O. Raineri, H. Resat and H. L. Friedman, *J. Chem. Phys.*, 1992, **96**, 3068.
107 (*a*) H. Resat, F. O. Raineri and H. L. Friedman, *J. Chem. Phys.*, 1992, **97**, 2618; (*b*) H. Resat, F. O. Raineri and H. L. Friedman, *J. Chem. Phys.*, 1993, **98**, 7277.
108 F. O. Raineri, B. C. Perng and H. L. Friedman, *Chem. Phys.*, 1994, **183**, 187.
109 (*a*) A. Chandra and B. Bagchi, *J. Chem. Phys.*, 1989, **91**, 1829; (*b*) A. Chandra and B. Bagchi, *J. Chem. Phys.*, 1989, **91**, 2594; (*c*) A. Chandra and B. Bagchi, *J. Chem. Phys.*, 1989, **91**, 3056; (*d*) A. Chandra and B. Bagchi, *J. Chem. Phys.*, 1990, **92**, 6833.
110 A. Chandra and B. Bagchi, *J. Phys. Chem.*, 1989, **93**, 6996.
111 M. Maroncelli and G. R. Fleming, *J. Chem. Phys.*, 1988, **89**, 5044.
112 C. P. Hsu, X. Song and R. A. Marcus, *J. Phys. Chem. B*, 1997, **101**, 2546.
113 A. Warshel and J.-K. Hwang, *J. Phys. Chem.*, 1986, **84**, 4938.
114 C. Silva, P. K. Walhout, K. Yokoyama and P. Barbara, *Phys. Rev. Lett.*, 1998, **80**, 1086.
115 J. C. Alfano, P. K. Walhout, Y. Kimura and P. F. Barbara, *J. Chem. Phys.*, 1993, **98**, 5996.
116 A. Kummrow, M. F. Emde, A. Baltuska, M. S. Pshenichnikov and D. A. Wiersma, *J. Phys. Chem. A*, 1998, **102**, 4172.
117 S. Bratos and J.-C. Leickman, *Chem. Phys. Lett.*, 1998, **261**, 117.
118 Y. Kimura, J. C. Alfano, P. K. Walhout and P. F. Barbara, *J. Phys. Chem.*, 1994, **98**, 3450.
119 W. Jarzeba, G. C. Walker, A. E. Johnson, M. A. Kahlow and P. F. Barbara, *J. Phys. Chem.*, 1998, **92**, 7039.
120 B. Zolotov, A. Gan, B. D. Feinberg and D. Huppert, *Chem. Phys. Lett.*, 1997, **265**, 418.
121 (*a*) B. Schwartz and P. J. Rossky, *J. Chem. Phys.*, 1994, **101**, 6902; (*b*) B. Schwartz and P. J. Rossky, *J. Chem. Phys.*, 1994, **101**, 6917; (*c*) B. Schwartz and P. J. Rossky, *Phys. Rev. Lett.*, 1991, **72**, 3283.
122 R. B. Barnett, U. Landman and A. Nitzan, *J. Chem. Phys.*, 1989, **90**, 4413.
123 E. Neria, A. Nitzan, R. B. Barnett and U. Landman, *Phys. Rev. Lett.*, 1991, **67**, 1011.
124 E. Neria and A. Nitzan, *J. Chem. Phys.*, 1989, **90**, 4413.

125 A. Staib and D. Borgis, *J. Chem. Phys.*, 1995, **103**, 2642.
126 P. L. Muino and P. R. Callis, *J. Chem. Phys.*, 1994, **100**, 4093.
127 (*a*) S. Roy and B. Bagchi, *J. Chem. Phys.*, 1993, **99**, 9938; (*b*) S. Roy and B. Bagchi, *J. Phys. Chem.*, 1994, **98**, 9207.
128 M. Cho, J. Y. Yu, T. Joo, Y. Nagasawa, S. A. Passino and G. R. Fleming, *J. Phys. Chem.*, 1996, **100**, 11944.
129 S. Passino, Y. Nagasawa and G. R. Fleming, *J. Chem. Phys.*, 1997, **107**, 6094.
130 W. P. de Boeij, M. S. Pshenichnikov and D. A. Wiersma, *Annu. Rev. Phys. Chem.*, 1998, **49**, 99.
131 A. P. Demchenko and A. S. Lodhokin, *Eur. Biophys. J.*, 1988, **15**, 569.
132 A. Chattopadhyay and S. Mukherjee, *Biochemistry*, 1993, **32**, 3804.
133 A. Chattopadhyay, S. Mukherjee and H. Raghuraman, *J. Phys. Chem. B*, 2002, **106**, 13002.
134 X. Song and D. Chandler, *J. Chem. Phys.*, 1998, **108**, 2594.
135 L. Onsager, *Can. J. Chem.*, 1977, **55**, 1819.
136 D. F. Calef and P. G. Wolynes, *J. Chem. Phys.*, 1983, **78**, 4145.
137 A. Chandra and B. Bagchi, *Chem. Phys. Lett.*, 1988, **151**, 47; A. Chandra and B. Bagchi, *Proc. Indian Acad. Sci. (Chem. Sci.)*, 1988, **100**, 353.
138 P. G. Wolynes, *J. Chem. Phys.*, 1987, **86**, 5133.
139 M. S. Wertheim, *J. Chem. Phys.*, 1971, **55**, 4291.
140 P. J. Rossky, *Annu. Rev. Phys. Chem.*, 1985, **36**, 321.
141 G. Stell, in *Statistical Mechanics Part A. Equilibrium Techniques*, ed. B. J. Berne, Plenum, New Work, 1977.
142 (*a*) I. Rips, J. Klafter and J. Jortner, *J. Chem. Phys.*, 1988, **88**, 3246; (*b*) I. Rips, J. Klafter and J. Jortner, *J. Chem. Phys.*, 1988, **89**, 4288.
143 (*a*) B. Bagchi and A. Chandra, *J. Chem. Phys.*, 1989, **90**, 7338; (*b*) B. Bagchi and A. Chandra, *Chem. Phys. Lett.*, 1989, **155**, 533.
144 (*a*) A. Chandra and B. Bagchi, *Chem. Phys. Lett.*, 1988, **151**, 47; (*b*) A. Chandra and B. Bagchi, *J. Phys. Chem.*, 1990, **94**, 3152.
145 S. Roy, S. Komath and B. Bagchi, *J. Chem. Phys.*, 1993, **99**, 3139.
146 (*a*) S. Roy and B. Bagchi, *J. Chem. Phys.*, 1993, **98**, 1310; (*b*) S. Roy and B. Bagchi, *J. Chem. Phys.*, 1994, **101**, 4150.
147 S. Komath and B. Bagchi, *J. Chem. Phys.*, 1993, **98**, 8987.
148 P. A. Madden and R. W. Impey, *Chem. Phys. Lett.*, 1986, **123**, 502.
149 R. W. Impey, P. A. Madden and R. W. Mcdonald, *Mol. Phys.*, 1982, **40**, 515.
150 P. A. Madden, in *Molecular Liquids: Dynamics and Interactions*, ed. A. J. Barnes, W. J. Orville-Thomas and J. Yarwood, Reidel Publ., Dordrecht, the Netherlands, 1984, p. 413.
151 See the articles in: *Water: A Comprehensive Treatise*, ed. F. Franks, Plenum, New York, 1972, vol. 1.
152 G. Nemethy and H. Scheraga, *J. Chem. Phys.*, 1964, **41**, 680.
153 See the articles in: *The Structure and Properties of Water*, ed. D. Eisenberg and W. Kauzman, Oxford University Press, London, 1969.
154 (*a*) G. E. Walrafen, *J. Chem. Phys.*, 1962, **36**, 1035; (*b*) G. E. Walrafen, *J. Chem. Phys.*, 1966, **44**, 1546; (*c*) G. E. Walrafen, *J. Chem. Phys.*, 1967, **47**, 114.
155 I. M. Svishchev and P. G. Kusalik, *J. Chem. Soc., Faraday Trans.*, 1994, **90**, 1405.
156 R. W. Zwanzig, *Phys. Rev.*, 1966, **144**, 170.
157 R. W. Zwanzig, in *Statistical Mechanics: New Concepts, New Problems, New Applications*, ed. S. A. Rice, K. F. Freed and J. C. Light, University of Chicago Press, Chicago, 1972.
158 M. Stratt, *Acc. Chem. Res.*, 1995, **28**, 201.
159 (*a*) B. M. Ladanyi and R. M. Stratt, *J. Phys. Chem.*, 1995, **99**, 2502; (*b*) B. M. Ladanyi and R. M. Stratt, *J. Phys. Chem.*, 1996, **100**, 1266.
160 M. Stratt and M. Cho, *J. Chem. Phys.*, 1994, **100**, 6700.
161 G. Goodyear, R. E. Larsen and R. M. Stratt, *Phys. Rev. Lett.*, 1996, **76**, 243.
162 R. E. Larsen, E. F. David, G. Goodyear and R. M. Stratt, *J. Chem. Phys.*, 1997, **107**, 524.
163 M. Buchner, B. M. Ladayni and R. M. Stratt, *J. Chem. Phys.*, 1992, **97**, 8522.
164 B. M. Ladayni, in *Electron and Ion transfer in Condensed Media*, ed. A. A. Koenyshev, M. Toshi, J. Ulstrup and M. P. Toshi, World Scientific, Singapore, 1997, p. 110.
165 H. Boyd, *J. Chem. Phys.*, 1961, **35**, 1281.
166 (*a*) R. Zwanzig, *J. Chem. Phys.*, 1963, **38**, 1603; (*b*) R. Zwanzig, *J. Chem. Phys.*, 1970, **52**, 3625.
167 B. J. Hubbard and L. Onsager, *J. Chem. Phys.*, 1977, **67**, 4850.
168 P. G. Wolynes, *Annu. Rev. Phys. Chem.*, 1980, **31**, 345.
169 P. G. Wolynes, *J. Chem. Phys.*, 1978, **68**, 473.
170 J. G. Kirkwood, *J. Chem. Phys.*, 1946, **14**, 180.
171 P. Colonomos and P. G. Wolynes, *J. Chem. Phys.*, 1979, **71**, 2644.
172 B. Bagchi, *J. Chem. Phys.*, 1991, **95**, 467.
173 R. Biswas, S. Roy and B. Bagchi, *Phys. Rev. Lett.*, 1995, **75**, 1098.
174 R. Biswas and B. Bagchi, *J. Chem. Phys.*, 1997, **106**, 5587.
175 R. Biswas and B. Bagchi, *J. Am. Chem. Soc.*, 1997, **119**, 5946.
176 M. Berkowitz and W. Wan, *J. Chem. Phys.*, 1987, **86**, 376.

177 L. Perera, U. Essman and M. L. Berkowitz, *J. Chem. Phys.*, 1995, **102**, 450.
178 (*a*) S. H. Lee and J. C. Rasiah, *J. Chem. Phys.*, 1994, **101**, 6964; (*b*) S. H. Lee and J. C. Rasiah, *J. Chem. Phys.*, 1996, **100**, 1420.
179 S. Efrima and M. Bixon, *J. Chem. Phys.*, 1979, **70**, 3531.
180 (*a*) L. D. Zusman, *Chem. Phys.*, 1980, **49**, 295; (*b*) L. D. Zusman, *Chem. Phys.*, 1983, **80**, 29; (*c*) L. D. Zusman, *Chem. Phys.*, 1988, **119**, 51; (*d*) L. D. Zusman, *Chem. Phys.*, 1990, **144**, 1.
181 J. T. Hynes, *J. Chem. Phys.*, 1986, **90**, 3701.
182 (*a*) R. F. Grote and J. T. Hynes, *J. Chem. Phys.*, 1980, **73**, 2715; (*b*) R. F. Grote and J. T. Hynes, *J. Chem. Phys.*, 1982, **77**, 3736.
183 H. Sumi and R. A. Marcus, *J. Chem. Phys.*, 1986, **84**, 4272.
184 E. A. Carter and J. T. Hynes, *J. Chem. Phys.*, 1991, **94**, 5961.
185 D. Huppert, V. Ittah and E. M. Kosower, *Chem. Phys. Lett.*, 1989, **159**, 267.
186 C. Chapman and M. Maroncelli, *J. Phys. Chem.*, 1991, **95**, 9095.
187 E. Neria and A. Nitzan, *J. Chem. Phys.*, 1994, **100**, 3855.
188 G. van der Zwan and J. T. Hynes, *Chem. Phys.*, 1991, **152**, 169.
189 (*a*) P. Debye and H. Falkenhagen, *Phys. Z.*, 1928, **29**, 121; (*b*) P. Debye and H. Falkenhagen, *Phys. Z.*, 1928, **29**, 401.
190 A. Chandra and G. N. Patey, *J. Chem. Phys.*, 1994, **100**, 1552.
191 A. Chandra, *Chem. Phys. Lett.*, 1995, **244**, 314.
192 A. Chandra, D. Jana and S. Bhattacharjee, *J. Chem. Phys.*, 1997, **106**, 2360.
193 F. Long, H. Lu and K. Eisenthal, *Phys. Rev. Lett.*, 1990, **64**, 1469.
194 Y. Gauduel, S. Pommeret, A. Migus and A. Antonetti, *J. Phys. Chem.*, 1991, **95**, 533.
195 Y. Gauduel, S. Pommeret and A. Antonetti, *J. Phys. Chem.*, 1993, **97**, 134.
196 (*a*) B. J. Schwartz and P. J. Rossky, *Phys. Rev. Lett.*, 1994, **72**, 3282; (*b*) B. J. Schwartz and P. J. Rossky, *J. Chem. Phys.*, 1994, **101**, 6917; (*c*) B. J. Schwartz and P. J. Rossky, *J. Chem. Phys.*, 1994, **101**, 6902; (*d*) B. J. Schwartz and P. J. Rossky, *J. Chem. Phys.*, 1996, **105**, 6997.
197 C. Silva, P. K. Walhout, K. Yokoyama and P. F. Barbara, *Phys. Rev. Lett.*, 1998, **80**, 1086.
198 S. Bratos, J.-C. Leicknam, D. Borgis and A. Staib, *Phys. Rev. E*, 1997, **55**, 7217.
199 See the articles in *Chem. Rev.* (Special Issue: Supercritical Fluids), 1999, **99**.
200 M. Re and D. Laria, *J. Phys. Chem. B*, 1997, **101**, 10494.
201 R. Biswas and B. Bagchi, *Chem. Phys. Lett.*, 1998, **290**, 223.
202 (*a*) N. Patel, R. Biswas and M. Maroncelli, *J. Phys. Chem. B*, 2002, **106**, 3306; (*b*) N. Patel and M. Maroncelli, *J. Chem. Phys.*, in press.
203 B. M. Ladanyi, personal communication.
204 X. Cheng and B. P. Schoenborn, *J. Mol. Biol.*, 1991, **220**, 381.
205 W. Gu and B. P. Schoenborn, *Proteins Struct. Funct. Genet.*, 1995, **22**, 20.
206 C. Rocchi, A. R. Bizzarri and S. Cannistraro, *Phys. Rev. E*, 1998, **57**, 3315.
207 M. Marchi, F. Sterpone and M. Ceccarelli, *J. Am. Chem. Soc.*, 2002, **124**, 6787.
208 M. Tarek and D. J. Tobias, *Biophys. J.*, 2000, **79**, 3244.
209 S. Boresch, P. Höchtl and O. Steinhauser, *J. Phys. Chem. B*, 2000, **104**, 8743.
210 E. J. Cohn, *Annu. Rev. Biochem.*, 1935, **4**, 53.
211 N. Nandi and B. Bagchi, *J. Phys. Chem. A*, 1998, **102**, 8217.
212 J. L. Oncley, *Chem. Rev.*, 1942, **30**, 433.
213 (*a*) J. G. Kirkwood and J. B. Shumaker, *Proc. Natl. Acad. Sci. USA*, 1952, **38**, 855; (*b*) J. G. Kirkwood and J. B. Shumaker, *Proc. Natl. Acad. Sci. USA*, 1952, **38**, 863.
214 B. Jacobson, *J. Am. Chem. Soc.*, 1955, **77**, 2919.
215 S. V. Ruffle, I. Michalarias, J.-C. Li and R. C. Ford, *J. Am. Chem. Soc.*, 2002, **124**, 565.
216 E. Dachwitz, F. Parak and M. Stockhausen, *Ber. Bunsen-Ges. Phys. Chem.*, 1989, **93**, 1454.
217 E. H. Grant, V. E. R. McClean, N. R. V. Nightingale, R. J. Sheppard and M. J. Chapman, *Bioelectromagnetics*, 1986, **7**, 151.
218 S. Mashimo, S. Kuwabara, S. Yagihara and K. Higasi, *J. Phys. Chem.*, 1987, **91**, 6337.
219 V. P. Denisov and B. Halle, *Faraday Discuss.*, 1996, **103**, 227.
220 V. Denisov, B. Halle, J. Peters and H. D. Horlein, *Biochemistry*, 1995, **34**, 9046.
221 D. W. Pierce and S. G. Boxer, *J. Phys. Chem.*, 1992, **96**, 5560.
222 J. S. Baskhin, G. McLendon, S. Mukamel and J. Marohn, *J. Phys. Chem.*, 1990, **94**, 4757.
223 B. Bagchi, 2002, unpublished work.
224 S. Sen, D. Sukul, P. Dutta and K. Bhattacharyya, *J. Phys. Chem. A*, 2001, **105**, 10635.
225 A. Geiger, A. Rahman and H. Stillinger, *J. Chem. Phys.*, 1979, **70**, 263.
226 S. Senapathy and S. Chandra, *J. Phys. Chem. B*, 2001, **105**, 5106.
227 J. Faeder and B. M. Ladanyi, *J. Phys. Chem. B*, 2001, **105**, 11148.
228 J. Faeder, M. V. Albert and B. M. Ladanyi, *Langmuir*, 2003, **19**, 2514.
229 (*a*) K. Watanabe and M. L. Klein, *J. Phys. Chem.*, 1989, **93**, 6897; (*b*) K. Watanabe and M. L. Klein, *J. Phys. Chem.*, 1991, **95**, 4158.
230 M. Sprik, U. Röthlisberger and M. L. Klein, *Mol. Phys.*, 1999, **97**, 355.
231 S. Pal, S. Balasubramanian and B. Bagchi, *J. Chem. Phys.*, 2002, **117**, 2852.

232 (*a*) S. Balasubramanian and B. Bagchi, *J. Phys. Chem. B*, 2001, **105**, 12529; (*b*) S. Balasubramanian and B. Bagchi, *J. Phys. Chem. B*, 2002, **106**, 3668.
233 S. Pal, S. Balasubramanian and B. Bagchi *Phys. Rev. E*, 2003, in press.
234 C. D. Bruce, M. L. Berowitz, L. Perera and M. D. E. Forbes, *J. Phys. Chem. B*, 2002, **106**, 3788.
235 C. D. Bruce, S. Senapati, M. L. Berkowitz, L. Perera and M. D. E. Forbes, *J. Phys. Chem. B*, 2002, **106**, 10902.
236 J. Shelley, K. Watanabe and M. L. Klein, *Int. J. Quantum Chem.: Quantum Biol. Symp.*, 1990, **17**, 103.
237 A. MacKerell, *J. Phys. Chem.*, 1995, **99**, 1846.
238 (*a*) T. Telgmann and U. Kaatze, *J. Phys. Chem. A*, 1998, **102**, 7758; (*b*) T. Telgmann and U. Kaatze, *J. Phys. Chem. A*, 1998, **102**, 7766.
239 D. M. Mittleman, M. C. Nuss and V. L. Colvin, *Chem. Phys. Lett.*, 1997, **275**, 332.
240 (*a*) M. D'Angelo, D. Fioretto, G. Onori, L. Palmieri and A. Santucci, *Phys. Rev. E*, 1996, **54**, 993; (*b*) M. D'Angelo, D. Fioretto, G. Onori, L. Palmieri and A. Santucci, *Phys. Rev. E*, 1995, **52**, 4620.
241 D. Toptygin, J. Svodva, I. Konopasek and L. Brand, *J. Chem. Phys.*, 1992, **96**, 7919.
242 W. R. Ware, *J. Phys. Chem. B.*, 1993, **103**, 563.
243 D. James and W. R. Ware, *Chem. Phys. Lett.*, 1985, **120**, 485.
244 N. Sarkar, A. Datta, S. Das and K. Bhattacharyya, *J. Phys. Chem.*, 1996, **100**, 15483.
245 A. Datta, D. Mandal, S. K. Pal and K. Bhattacharyya, *J. Mol. Liq.*, 1998, **77**, 121.
246 H. H. Paradies, *J. Phys. Chem.*, 1980, **84**, 599.
247 S. S. Berr, *J. Phys. Chem.*, 1987, **91**, 4760.
248 S. S. Berr, M. J. Coleman, R. R. M. Jones and J. S. Johnson, *J. Phys. Chem.*, 1986, **90**, 5766.
249 S. S. Berr, E. Caponetti, R. R. M. Jones, J. S. Johnson and L. J. Magid, *J. Phys. Chem.*, 1986, **90**, 5766.
250 G. Jones, II, W. P. Jackson and C. Y. Choi, *J. Phys. Chem.*, 1985, **89**, 294.
251 N. Sarkar, K. Das, A. Datta, S. Das and K. Bhattacharyya, *J. Phys. Chem.*, 1996, **100**, 10523.
252 J. S. Lundgren, M. P. Heitz and F. V. Bright, *Anal. Chem.*, 1995, **67**, 3775.
253 D. Mandal, A. Datta, S. K. Pal and K. Bhattacharyya, *J. Phys. Chem. B*, 1998, **102**, 9070.
254 D. M. Willard, R. E. Riter and N. E. Levinger, *J. Am. Chem. Soc.*, 1998, **120**, 4151.
255 R. E. Riter, E. P. Undiks and N. E. Levinger, *J. Am. Chem. Soc.*, 1998, **120**, 6062.
256 R. E. Riter, D. M. Willard and N. E. Levinger, *J. Phys. Chem. B*, 1998, **102**, 2705.
257 R. E. Riter, E. P. Undiks, J. R. Kimmel, D. D. Pant and N. E. Levinger, *J. Phys. Chem. B*, 1998, **102**, 7931.
258 H. Shirota and K. Horie, *J. Phys. Chem. B*, 1999, **103**, 1437.
259 A. Datta, S. K. Pal, D. Mandal and K. Bhattacharyya, *J. Phys. Chem. B*, 1998, **102**, 6114.
260 R. Cassol, M.-T. Ge, A. Ferrarini and J. H. Freed, *J. Phys. Chem. B*, 1997, **101**, 8782.
261 M. M. Sung-Suh and L. Kelvan, *J. Phys. Chem. A*, 1997, **101**, 1414.
262 A. Jutila and P. K. Kinninen, *J. Phys. Chem. B*, 1997, **101**, 7635.
263 M. M. Teeter, A. Yamano, B. Stec and U. Mohanty, *Proc. Natl. Acad. Sci. USA*, 2001, **98**, 11242.
264 M. Tarek and D. J. Tobias, *Phys. Rev. Lett.*, 2002, **88**, 138101–1.
265 A. L. Lee and A. J. Wand, *Nature (London)*, 2001, **411**, 501.
266 B. F. Rasmussen, A. M. Stock, D. Ringe and G. A. Petsko, *Nature (London)*, 1992, **357**, 423.
267 M. Ferrand, A. J. Dianoux, W. Petry and G. Zaccai, *Proc. Natl. Acad. Sci. USA*, 1993, **90**, 9668.
268 C. A. Angell, *Proc. Natl. Acad. Sci. USA*, 1995, **92**, 6675.
269 C. A. Angell, *Nature (London)*, 1999, **398**, 492.
270 S. Balasubramanian, S. Pal and B. Bagchi, unpublished work.
271 D. Ringe, *Curr. Biol.*, 1995, **5**, 825.
272 S. Zou, J. S. Baskin and A. H. Zewail, *Proc. Natl. Acad. Sci. USA*, 2002, **99**, 9625.
273 C. J. Camacho, S. R. Kimura, C. DeLisi and S. Vajda, *Biophys. J.*, 2000, **78**, 1094.